PROSPECTS FOR THE OBSERVABILITY OF THE $\boldsymbol{WH}$ AND $\boldsymbol{ZH}$, $\boldsymbol{H \to b\bar{b}}$ CHANNEL IN 14 TeV $\boldsymbol{pp}$ AND 2 TeV $\boldsymbol{p\bar{p}}$ COLLISIONS ($\boldsymbol{E_{\mathrm{T}}^{\mathrm{miss}} + b\bar{b}}$ FINAL STATE)*

Elżbieta Richter-Wąs

Institute of Computer Science, Jagellonian University
Institute of Nuclear Physics
Kawiory 26a, 30-055 Kraków, Poland
CERN, EP Division, 1211 Geneva 23, Switzerland

(Received August 1, 2000)

A detailed study of the associated Standard Model Higgs boson production in 14 TeV pp (LHC) and 2 TeV $p\bar{p}$ (Tevatron) collisions, WH/ZH with $H \to b\bar{b}$ decay and $E_{\mathrm{T}}^{\mathrm{miss}} + b\bar{b}$ signature, is presented for a benchmark value of the Higgs boson mass, $m_H = 100$ GeV. The observation of these events with ATLAS at LHC is considered not to be feasible because of the overwhelming background from QCD jet events. Contrary, this signature is claimed to be promising for a Higgs boson discovery in the mass range of 90–140 GeV at the Tevatron $p\bar{p}$ collider.The aim of this paper is to provide several details which lead to a quantitative comparison in a consistent framework of the physics potential for this signature in both colliding scenarios. The emphasis is put on the differences in the expected signal and backgrounds rates and the background composition. Together with a similar study presented on the WH/ZH production with $\ell b\bar{b}$ and $\ell\ell b\bar{b}$ final states, it covers most sensitive signatures discussed in the Tevatron report for the Higgs searches in the mass range 90–140 GeV.

PACS numbers: 14.80.Bn, 14.80.Cp, 14.65.Ha

* Supported in part by Polish State Committee grant KBN 2P03B11819, by Polish-American Maria Skłodowska-Curie Joint Fund II in cooperation with PAA and DOE under project PAA/DOE-97-316 and Polish-French Collaboration within IN2P3.

CONTENTS

1 Introduction 1975
2 Expected production rates 1976
3 Simulation procedure and selection criteria 1978
4 Signal and backgrounds in 14 TeV pp collision 1979
4.1 ZH and WH signals 1979
4.2 ZZ and WZ resonant backgrounds 1980
4.3 Zjj and Wjj continuum backgrounds 1982
4.4 Top pair and single top background 1984
4.5 Total signal and W, Z, single t and top-pair backgrounds 1986
4.6 The QCD continuum background 1987
4.7 Conclusions 1993
5 2 TeV $p\bar{p}$ versus 14 TeV pp 1993
5.1 ZH and WH signals 1994
5.2 ZZ and WZ resonant background 1996
5.3 Zjj and Wjj continuum background 1997
5.4 Top pair and single top background 1998
5.5 Total signal and W, Z, single top and top-pair backgrounds . . 2001
5.6 The QCD continuum background 2002
5.7 Conclusions 2010
5.8 Comparison with results from [2] 2010
6 Conclusions 2017

1. Introduction

If the mass of the Standard Model Higgs boson is lighter than 2 m_W the $H \to b\bar{b}$ decay mode is dominant with a branching ratio of $\sim 90\%$. The observation of such a characteristic signature would be important for both the Higgs boson discovery and for the determination of the nature of any resonance observed in this mass region. Since the direct production, $gg \to H$ with $H \to b\bar{b}$, cannot be efficiently triggered nor extracted as a signal above the huge QCD two-jet background, the associated production with a W- or Z-boson or a $t\bar{t}$ pair remains as the only possible process to observe a signal from the $H \to b\bar{b}$ decays. The final state of the decaying Z or W (produced directly or from $t\bar{t}$) might provide a handle to extract a signal above the overwhelming QCD background, thanks to the isolated lepton or large missing energy in the final state.

Prospects for the $H \to b\bar{b}$ observability in the associated production with a W or a $t\bar{t}$ pair have been discussed already in several documents of the ATLAS Collaboration [1, 4]. The production in association with a top pair, $t\bar{t}H$ has been established as a valuable discovery channel [5], while the sensitivity to the WH production, studied already in [6], has been confirmed recently [3] to be rather weak.

The ZH production has not been studied in details before by the ATLAS Collaboration as it is not considered as having a discovery potential [1]. With the $Z \to \ell\ell$ decay, leading to the $\ell\ell bb$ signature, it would provide initial rates which are about six times lower than the WH rates. The signal-to-background ratio is not expected to be significantly better, compared to the WH channel [3]. With the $Z \to \nu\nu$ decay, leading to the $E_{\mathrm{T}}^{\mathrm{miss}} + b\bar{b}$ signature, it would be difficult to trigger efficiently on. In addition, it would suffer from potentially very large experimental backgrounds given the rather low average missing energy, $E_{\mathrm{T}}^{\mathrm{miss}}$, expected for the signal events.

Since this last channel has been discarded as a promising one at the LHC, it is important to understand why it is discussed as a sensitive one at the upgraded Tevatron [2]. Although some clear advantages might come from the reduced center-of-mass energy (events being more central at lower energy, less hadronic activity in the event, relative magnitude of the initial $t\bar{t}$ cross-section), it is obvious that for the same assumed integrated luminosity the expected rates would be substantially lower at the Tevatron than at the LHC.

In this paper the WH/ZH associated production with $E_{\mathrm{T}}^{\mathrm{miss}} + bb$ signature is studied. A rather detailed evaluation of the signal and background is presented first for the LHC environment and then a detailed comparison of the 2 TeV $p\bar{p}$ and 14 TeV pp scenarios is carried out. Particular emphasis is put on the understanding and evaluation of the QCD background to this signature. An attempt is also made to break down the differences in the numbers estimated here for the expected signal and background rates and those specified in the Tevatron report [2].

2. Expected production rates

The studied signature consists of two identified b-jets accompanied by the missing transverse energy. The irreducible background comes from the processes with the true isolated missing energy from W or Z decays. However, the key point for the observation of this channel is the capability to suppress the potentially several order of magnitudes larger QCD background with fake or true missing transverse energy.

Table I shows the production cross-sections for the signal and various reference backgrounds as calculated with PYTHIA 5.7 Monte Carlo and CTEQ2L structure functions. Although this parametrisation for the structure functions is a bit outdated, it can still be used for the benchmark-like comparison as presented in this paper. The $H, Z \to b\bar{b}$, $W \to l\nu (l = e, \mu)$ and $Z \to \nu\nu$ branching ratios are included. The W+jet, Z+jet and QCD cross-sections are quoted for the hard process transverse momenta, $p_{\rm T}^{\rm hard}$, in a specified ranges. To this signature also events from $Z \to \tau\tau$ and $W \to \tau\nu$ would contribute significantly. These are included in the final estimates of the expected rates.

The dominant uncertainties on the expected rates arise from the higher order corrections and, to a smaller extend, from the structure function parameterisation. A larger uncertainty is expected for W+jet and Z+jet production as the multijet final state is generated with the parton shower approach only (see also discussion in [3]).

In all cases the Monte-Carlo statistics used in this study is very high. Typically 10^5 events were simulated for each background process while in the case of the W+jet, Z+jet processes, 5×10^6 events were simulated in each $p_{\rm T}^{\rm hard}$ range. For the QCD background around 10^8 events were simulated in total, sampled with grids in $p_{\rm T}^{\rm hard}$ of 5 GeV and 10 GeV.

As shown in Table I, signal and resonant background cross-sections are almost factor 10 higher in 14 TeV pp collision. Inclusive rates for Z+jet, W+jet and QCD production are also higher by a comparable factor and the ratio increases with rising threshold on the transverse momenta of the hard scattering process.

TABLE I

Production cross-sections for the ZH /WH signal and background processes leading to the $E_{\mathrm{T}}^{\mathrm{miss}} + b\bar{b}$ final state signature in the 14 TeV pp and 2 TeV $p\bar{p}$ collision. Branching ratios of $Z \to \nu\nu$, $W \to \ell\nu$ ($l = e, \mu$) and $H \to b\bar{b}$ are included.

Process	pp at 14 TeV σ [pb]	$p\bar{p}$ at 2 TeV σ [pb]	Ratio
ZH, $m_H = 100$ GeV (with $Z \to \nu\nu$)	0.21	0.023	10
WH, $m_H = 100$ GeV (with $W \to \ell\nu$)	0.40	0.042	10
ZZ (with one $Z \to \nu\nu$)	0.69	0.060	10
WZ (with $W \to \ell\nu$)	0.86	0.083	10
$t\bar{t}$ (with at least one $W \to \ell\nu$)	228	2.62	87
tq (with $W \to \ell\nu$)	44.4	0.565	78
$Z +$ jet (with $Z \to \nu\nu$)			
$p_{\mathrm{T}}^{\mathrm{hard}} = 10$–$30$ GeV	3.4×10^3	2.8×10^2	12
$p_{\mathrm{T}}^{\mathrm{hard}} = 30$–$50$ GeV	8.3×10^2	5.3×10^1	16
$p_{\mathrm{T}}^{\mathrm{hard}} = 50$–$100$ GeV	5.1×10^2	2.4×10^1	21
$p_{\mathrm{T}}^{\mathrm{hard}} = 100$–$200$ GeV	1.1×10^2	3.2×10^0	34
$p_{\mathrm{T}}^{\mathrm{hard}} => 200$ GeV	1.3×10^1	0.1×10^0	100
$W +$ jet (with $W \to \ell\nu$)			
$p_{\mathrm{T}}^{\mathrm{hard}} = 10$–$30$ GeV	1.1×10^4	9.7×10^2	11
$p_{\mathrm{T}}^{\mathrm{hard}} = 30$–$50$ GeV	2.7×10^3	1.7×10^2	16
$p_{\mathrm{T}}^{\mathrm{hard}} = 50$–$100$ GeV	1.5×10^3	7.4×10^1	20
$p_{\mathrm{T}}^{\mathrm{hard}} = 100$–$20$ GeV	3.2×10^2	8.3×10^0	38
$p_{\mathrm{T}}^{\mathrm{hard}} => 200$ GeV	3.5×10^1	0.3×10^0	130
QCD jets			
$p_{\mathrm{T}}^{\mathrm{hard}} = 10$–$30$ GeV	5.9×10^9	5.0×10^8	12
$p_{\mathrm{T}}^{\mathrm{hard}} = 30$–$50$ GeV	1.3×10^8	1.0×10^6	24
$p_{\mathrm{T}}^{\mathrm{hard}} = 50$–$100$ GeV	2.1×10^7	5.8×10^5	36
$p_{\mathrm{T}}^{\mathrm{hard}} = 100$–$200$ GeV	1.4×10^6	1.7×10^4	82
$p_{\mathrm{T}}^{\mathrm{hard}} => 200$ GeV	7.4×10^4	2.2×10^2	340

3. Simulation procedure and selection criteria

In the first step, signal and W, Z, $t\bar{t}$ originated backgrounds are analysed with the selection which would be adequate to extract a signal above the irreducible and reducible backgrounds with true isolated missing energy from heavy bosons decay to neutrinos. Such a selection is not sufficient to suppress the reducible QCD background. A complementary selection criteria, which might reject some fraction of the huge reducible background and still remains efficient for the signal events are discussed in Section 4.6.

The standard selection criteria for the $E_{\mathrm{T}}^{\mathrm{miss}} + b\bar{b}$ final state, as denoted in Tables[1] below, are the following ones:

- $E_{\mathrm{T}}^{\mathrm{miss}}$: The missing transverse energy, calculated from the total sum of the deposited energies, is required to be larger than 30 GeV.

- *"LVL1" selection*: At present no stand-alone $E_{\mathrm{T}}^{\mathrm{miss}}$ trigger is foreseen with LHC. There, it is proposed only the combined $E_{\mathrm{T}}^{\mathrm{miss}}$ + jet trigger, which also requires presence of a hard-p_{T} jet. Presently, the trigger threshold foreseen by the LVL1 trigger menu of ATLAS [10] is $E_{\mathrm{T}}^{\mathrm{miss}} > 50$ GeV. It has to be accompanied by at least one hard jet with $p_{\mathrm{T}}^{\mathrm{jet}} > 50$ GeV and $|\eta| < 3.2$. In the results presented below, trigger efficiency is not included and the thresholds are set on the jets transverse momenta and missing transverse energy reconstructed from the fast simulation.

- *2b-jets:* 2b-labelled jets with[2] $p_{\mathrm{T}} > 25$ GeV and pseudorapidity $|\eta| < 2.5$.

- *Jet-veto:* Veto events with any additional jet of $p_{\mathrm{T}} > 30$ GeV and $|\eta| < 5.0$.

- *Lepton-veto:* Veto events with an isolated lepton with $p_{\mathrm{T}} > 6$ GeV and $|\eta| < 2.5$ GeV.

- *Mass window:* Is chosen as respective for the resolution σ=10% m_H, namely the window $m_{bb} = 100 \pm 20$ GeV. Acceptance in the mass window is of 85% for signal events and 73% for resonant ZZ/WZ backgrounds. This can be considered as realistic, as the acceptance of 82% in the mass window 100 $\pm$ 20 GeV was achieved for signal events

[1] In the Tables which show cumulative acceptance, the acceptance in the m_{bb} mass window and b-tagging efficiency is not included neither for signal nor for the backgrounds. This acceptance and efficiency are included in Tables which give expected number of events for an integrated luminosity of 30 fb^{-1}.

[2] This threshold is set on the recalibrated jets energies [3]. It corresponds to 10 GeV threshold on the 100% efficient calorimeter reconstruction in cone $\Delta R = 0.4$ and 15 GeV threshold after applying Gaussian smearing with $50\%/\sqrt{E}$ resolution [11].

with the full simulation and selection without jet veto [1]. As discussed in [3], jet-veto leads to better acceptance inside mass window, as events with abundant radiation are not passing this selection.

- *b-tagging:* A nominal b-tagging efficiency of 60% with a rejection of 10 and 100 against c-jets and light-jets respectively is adopted. Some indication on the impact of the p_{T} and $|\eta|$ dependence of the b-tagging efficiency on the signal observability can be found in [1, 8].

4. Signal and backgrounds in 14 TeV *pp* collision

4.1. ZH and WH signals

Cumulative acceptances for signal events from the ZH and WH production processes are given in Table II and the expected number of events for an integrated luminosity of 30 fb^{-1} are shown in Table III.

TABLE II

For signal events, expected cumulative acceptances of the selection criteria. The b-tagging efficiency and acceptance in the mass window are not included.

Cumulative acceptance	$E_{\mathrm{T}}^{\mathrm{miss}} > 30$ GeV	"LVL1" selection
	ZH, $Z \to \nu\nu$	
$E_{\mathrm{T}}^{\mathrm{miss}}$+ lepton veto	77.3%	49.4%
+ 2 b-labelled jets	31.2%	22.3%
+ jet veto 30 GeV	15.2%	10.5%
	ZH, $Z \to \tau\tau$	
$E_{\mathrm{T}}^{\mathrm{miss}}$+ lepton veto	26.3%	10.4%
+ 2 b-labelled jets	9.3%	4.2%
+ jet veto 30 GeV	0.8%	0.4%
	WH, $W \to \tau\nu$	
$E_{\mathrm{T}}^{\mathrm{miss}}$+ lepton veto	52.3%	26.7%
+ 2 b-labelled jets	19.8%	12.1%
+ jet veto 30 GeV	4.2%	2.3%
	WH, $W \to \ell\nu$	
$E_{\mathrm{T}}^{\mathrm{miss}}$+ lepton veto	16.3%	7.2%
+ 2 b-labelled jets	4.0%	2.7%
+ jet veto 30 GeV	1.2%	0.7%

TABLE III

For an integrated luminosity of 30 fb^{-1}, expected number of events from the ZH and WH signal inside the mass window, after all cuts and including nominal b-tagging efficiency.

Process	$E_{\mathrm{T}}^{\mathrm{miss}} > 30$ GeV		"LVL1" selection	
	No jet veto	With jet veto	No jet veto	With jet veto
ZH with $Z \to \nu\nu$	601	293	430	202
ZH with $Z \to \tau\tau$	29	3	13	1
WH with $W \to \tau\nu$	363	77	222	42
WH with $W \to \ell\nu$	147	44	99	25
Total signal	1140	417	764	270

The selection criteria are chosen to reduce the $W \to \ell\nu$ originated background with lepton-veto and the $W \to \tau\nu$, $Z \to \tau\tau$ originated ones with jet-veto. Effectively, the acceptance for signal events is more than 3 times higher for the associated production with $W \to \tau\nu$ than with $W \to \ell\nu$ production. For the associated production with $Z \to \tau\tau$ acceptance is very low.

Depending on the details of the selection criteria, see Table III, the ZH with $Z \to \nu\nu$ channel contributes around 50% (no jet-veto) or 70% (with jet-veto) to the total signal rates. Significant contribution, respectively 32% or 18%, comes also from the WH with $W \to \tau\nu$ channel.

4.2. ZZ and WZ resonant backgrounds

The acceptance for the selection criteria is somewhat lower for the resonant WZ and ZZ channels than for the respective signal processes.

The total number of expected events inside the mass window is almost 2 times higher than from the signal itself. Effectively, the presence of the signal will broader and increase the resonant mass peak expected from the ZZ and WZ events, as already discussed in [3] for $\ell b\bar{b}$ and $\ell\ell b\bar{b}$ signatures. The capability for extracting Higgs signal peak itself would relay on the capability for the calibration of the resonant and continuum backgrounds with the data and Monte Carlo simulations. The uncertainties from systematic errors will be limited by the availability of control channels.

TABLE IV

The same as Table II but for ZZ and WZ events.

Cumulative acceptance	$E_T^{miss} > 30$ GeV	"LVL1" selection
	ZZ with $Z \to \nu\nu$	
E_T^{miss}+ lepton veto	68.5%	37.1%
+ 2 b-labelled jets	24.5%	15.0%
+ jet veto 30 GeV	12.0%	6.9%
	ZZ with $Z \to \tau\tau$	
E_T^{miss}+ lepton veto	20.7%	7.0%
+ 2 b-labelled jets	6.8%	2.6%
+ jet veto 30 GeV	0.7%	0.3%
	WZ with $W \to \tau\nu$	
E_T^{miss}+ lepton veto	49.7%	21.4%
+ 2 b-labelled jets	16.5%	8.4%
+ jet veto 30 GeV	3.9%	2.1%
	WZ with $W \to \ell\nu$	
E_T^{miss}+ lepton veto	17.9%	6.9%
+ 2 b-labelled jets	5.8%	2.6%
+ jet veto 30 GeV	1.8%	0.9%

TABLE V

The same as Table III but for ZZ and WZ events.

Expected events	$E_T^{miss} > 30$ GeV		"LVL1" selection	
	No jet veto	With jet veto	No jet veto	With jet veto
ZZ with $Z \to \nu\nu$	1370	670	840	385
ZZ with $Z \to \tau\tau$	60	10	25	5
WZ with $W \to \tau\nu$	580	135	295	70
WZ with $W \to \ell\nu$	400	125	180	60
Total reson. bgd	2410	940	1340	520

4.3. Zjj and Wjj continuum backgrounds

• **Zjj continuum background**

The Zjj background has been simulated using $gq \to Z + q$, $q\bar{q} \to Z + g$ matrix element calculations and parton shower, as implemented in PYTHIA Monte Carlo. As already discussed in [3], the dominant $gg \to Zb\bar{b}$ contribution is realised through the evolution of the structure functions and not by the matrix element calculations. The results presented below are therefore very likely underestimating the contribution from this subprocess. A more detailed discussion on the heavy flavour composition of this background is given in [3]. The fraction of the Zbb events in the total Zjj background varies with the selection criteria, reaching ± 90% for the "LVL1" selection with jet-veto.

TABLE VI

For the Zjj events, cumulative acceptance for events already filtered on 2 reconstructed jets in $|\eta| < 2.5$ and on the transverse missing energy $E_{\mathrm{T}}^{\mathrm{miss}} > 30$ GeV. The acceptance is given for merged together samples generated in different $p_{\mathrm{T}}^{\mathrm{hard}}$ bins.

Cumulative acceptance	$E_{\mathrm{T}}^{\mathrm{miss}} > 30$ GeV	"LVL1" selection
$E_{\mathrm{T}}^{\mathrm{miss}}$ + lepton veto	(filter) 82.2%	(filter) 59.4%
+ 2 b-labelled jets	filter	filter
+ jet veto 30 GeV	23.9%	15.7%

Only the Zjj with $Z \to \nu\nu$ background was simulated. The additional contribution from Zjj events with $Z \to \tau\tau$ was estimated assuming that the ratio of the acceptances for these two channels is similar to those for the ZZ background. The contribution to the total Zjj background would be therefore 5% (resp. 1%) for selection without jet-veto (resp. with jet-veto) of the background from the Zjj with $Z \to \nu\nu$. As nevertheless the much larger uncertainties are related to the estimation of the total Zjj background, the $Z \to \tau\tau$ contribution is neglected in the further evaluation.

After all selection cuts, the fraction of the Zbb events in the accepted Zjj sample is systematically higher than that fraction in the $\ell\ell b\bar{b}$ analysis [3].

• **Wjj continuum background**

Similarly to the Zjj case, also this background was simulated using a parton shower approach in PYTHIA. More detailed discussion on the jets flavour composition and comparison with the matrix element (ME) calculations for the $q\bar{q} \to Wbb$ subprocesses can be found in [3]. After all selection cuts, the fraction of the Wbb events in accepted Wjj sample is systematically higher than in the case of the $\ell b\bar{b}$ analysis [3].

Only the Wjj with $W \to \ell\nu$ background was simulated. The additional contribution from the Wjj events with $W \to \tau\nu$ was estimated with the assumption that the ratio of acceptances for these two channels is similar to the respective ratio for the WZ background with the $W \to \tau\nu$ and $W \to \ell\nu$ decays.

TABLE VII

The same as Table II but for W+jet events ($W \to \ell\nu$) already filtered on 2 reconstructed jets with $|\eta| < 2.5$. Acceptance is given for merged together samples generated in different $p_{\mathrm{T}}^{\mathrm{hard}}$ bins.

Cumulative acceptance	$E_{\mathrm{T}}^{\mathrm{miss}} > 30$ GeV	"LVL1" selection
$E_{\mathrm{T}}^{\mathrm{miss}}$ + lepton veto	17.2%	10.9%
+ 2 b-labelled jets	filter	filter
+ jet veto	3.0%	2.1%

• **Total continuum background from Zjj and Wjj events**

The total continuum background is dominated by the true $Wb\bar{b}$ and $Zb\bar{b}$ events.

TABLE VIII

The same as Table III but for Zjj and Wjj events.

Expected events	$E_{\mathrm{T}}^{\mathrm{miss}} > 30$ GeV		"LVL1" selection	
	No jet veto	With jet veto	No jet veto	With jet veto
	Zjj with $Z \to \nu\nu$			
bb	25000	14000	13300	7000
(jb, jc, bc, cc, jj)	2700	1800	1700	800
	Wjj with $W \to \tau\nu$			
bb	8600	1600	3700	1100
(jb, jc, bc, cc, jj)	2200	700	900	300
	Wjj with $W \to \ell\nu$			
bb	6000	1500	2300	1000
(jb, jc, bc, cc, jj)	1500	600	600	200

4.4. Top pair and single top background

• Top pair background

This channel results in a $WWb\bar{b}$ final state. The decays $W \to \tau\nu$ or $W \to \ell\nu$ lead to the true missing energy. The combination of the lepton-veto and jet-veto leads to a huge rejection for this background. The cumulative acceptance, as shown in Table IX, is 0.16% for $W \to \tau\nu$ and 0.09% for $W \to \ell\nu$ decays of at least one W from the top-pair. For example, the rejection of events with a $W \to \ell\nu$ is factor 20 higher than in the $\ell b\bar{b}$ analysis (see Section 2 of [3]). After jet-veto, the expected background from the $t\bar{t}$ events is at most only factor 2 higher than the expected signal itself. This background therefore will not be the severe one for the $E_{\mathrm{T}}^{\mathrm{miss}} + b\bar{b}$ signature.

TABLE IX

For the $t\bar{t}$ background, cumulative acceptances of the selection criteria.

Cumulative acceptance	$E_{\mathrm{T}}^{\mathrm{miss}} > 30$ GeV	"LVL1" selection
	at least one $W \to \tau\nu$	
$E_{\mathrm{T}}^{\mathrm{miss}}$+ lepton veto	47.9%	34.3%
+ 2 b-labelled jets	27.0%	19.5%
+ jet veto 30 GeV	0.16%	0.13%
	at least one $W \to \ell\nu$	
$E_{\mathrm{T}}^{\mathrm{miss}}$+ lepton veto	12.4%	8.7%
+ 2 b-labelled jets	6.5%	4.6%
+ jet veto 30 GeV	0.09%	0.06%

• *tb*, *tc* continuum background

This channel results in a Wb final state with an additional b, c or light quark from the hard process. The decays $W \to \tau\nu$ or $W \to \ell\nu$ lead to the true transverse missing energy. Combination of the lepton-veto and jet-veto leads to a huge rejection. The cumulative acceptance, as shown in Table X, is 0.4% for $W \to \tau\nu$ and 0.15% for $W \to \ell\nu$ decays for events already filtered on the presence of at least 2 b- or c- labelled jets. For example, the rejection of the $W \to \ell\nu$ events is a factor of 17 higher than in the $\ell b\bar{b}$ analysis (see Section 2.3. of [3]). With the jet-veto being applied, expected number of the tb, tc events is almost 8 times lower than the expected number of signal events. This background is more than a factor 15 smaller than the $t\bar{t}$ background and contribute marginally to the backgrounds for the $E_{\mathrm{T}}^{\mathrm{miss}} + b\bar{b}$ signature.

• **$W^* \to tb$ background**

This channel results in a $Wb\bar{b}$ final state. The decays $W \to \tau\nu$ or $W \to \ell\nu$ lead to a presence of the true missing energy. Combination of the lepton-veto and jet-veto leads to the huge rejection factor for this channel. This background was generated with HERWIG Monte Carlo and only the $W \to \ell\nu$ decay mode could be simulated with the available version. To estimate the $W \to \tau\nu$ contribution it was assumed that this channel behaves similarly to the tb, tc one, see Table X, so that the acceptance before jet-veto is higher by factor 4.7 and after jet-veto by factor 2.7 for the $W \to \tau\nu$ with respect to the $W \to \ell\nu$ final state.

TABLE X

For the single top production, cumulative acceptances of the selection criteria for events already filtered on at least 2 b- or c-labelled jets.

Cumulative acceptance	$E_{\mathrm{T}}^{\mathrm{miss}} > 30$ GeV	"LVL1" selection
	$W \to \tau\nu$	
$E_{\mathrm{T}}^{\mathrm{miss}}$ + lepton veto	57.7%	34.5%
+ 2 b-labelled jets	27.1%	17.2%
+ jet veto 30 GeV	0.4%	0.2%
	$W \to \ell\nu$	
$E_{\mathrm{T}}^{\mathrm{miss}}$ + lepton veto	11.2%	6.4%
+ 2 b-labelled jets	5.8%	3.3%
+ jet veto 30 GeV	0.15%	0.08%

TABLE XI

For the $W^* \to tb$ process with $W \to \ell\nu$, cumulative acceptances of the selection criteria.

Cumulative acceptance	$E_{\mathrm{T}}^{\mathrm{miss}} > 30$ GeV	"LVL1" selection
$E_{\mathrm{T}}^{\mathrm{miss}}$ + lepton veto	19.0%	10.5%
+ 2 b-labelled jets	7.4%	4.6%
+ jet veto 30 GeV	2.0%	1.2%

TABLE XII

The same as Table III but for the single and top-pair production.

Expected events	$E_{\mathrm{T}}^{\mathrm{miss}} > 30$ GeV		"LVL1" selection	
	No jet veto	With jet veto	No jet veto	With jet veto
	$t\bar{t}$			
With $W \to \tau\nu$	72500	340	52500	270
With $W \to \ell\nu$	32500	440	23500	270
Total	105000	780	76000	540
	$W^* \to tb$			
With $W \to \tau\nu$	440	30	280	20
With $W \to \ell\nu$	210	60	130	40
Total	650	90	410	60
	$tb,\ tc$ continuum			
With $W \to \tau\nu$	1600	30	970	15
With $W \to \ell\nu$	700	20	330	5
Total	2300	50	1300	20

Cumulative acceptance, as shown in Table XI, is of 2.0% for the $W \to \ell\nu$ decay mode. Rejection for these events is therefore factor 11 higher than in the $\ell b\bar{b}$ analysis (see Section 2.3.3 of [3]). After jet-veto, expected number of the $W^* \to tb$ events is factor 4 smaller than the expected number of the signal events. This background will therefore contribute marginally to the backgrounds for the $E_{\mathrm{T}}^{\mathrm{miss}} + b\bar{b}$ signature.

Table XII shows summary on the expected background from the top events.

4.5. Total signal and W, Z, single t and top-pair backgrounds

The expected number of signal and background events with Z or W in the final state is given in Table XIII for the selection without and with the jet veto. If the total background to this channel were dominated by the events with true transverse missing energy, E_{T}^{ν}, from W or Z decays, a sensitivity of 3σ only could be expected for an integrated luminosity of 30 fb^{-1}. The suppression of the single top and the $t\bar{t}$ backgrounds with jet-veto leads to a more favourable signal-to-background ratio. This selection can probably be optimised even further. The signal-to-resonant-background ratio, here only 1 : 2, is however less favourable than for the ℓbb signature. Obviously the jet-veto combined with the lepton-veto suppresses more efficiently the Wjj than Zjj backgrounds. Just, with the jet-veto at 30 GeV, the Zbb channel with $Z \to \nu\nu$ becomes the dominant background source with the real $E_{\rm T}^{\nu}$ from W or Z production.

TABLE XIII

For an integrated luminosity of 30 fb^{-1}, expected number of signal and background events after all cuts. The nominal b-tagging efficiency is assumed. The $Z \to \nu\nu$, $Z \to \tau\tau$, $W \to \ell\nu$ and $W \to \tau\nu$ decays are included.

Process	$E_{\rm T}^{\rm miss} > 30$ GeV		"LVL1" selection	
	No jet veto	Jet veto 30 GeV	No jet veto	Jet veto 30 GeV
ZH	630	296	443	203
WH	510	121	321	67
Total signal	1140	417	764	270
ZZ	1430	680	865	390
WZ	980	260	475	130
Res. bgd (W, Z)	2410	940	1340	520
tt	105000	780	76000	540
single t	2950	140	1700	80
Zjj (bb)	25000	14000	13300	7000
Zjj (other)	2700	1800	1700	800
Wjj (bb)	14600	3100	6000	2100
Wjj (other)	3700	1300	1500	500
Cont. bgd (W,Z,t,$t\bar{t}$)	154000	21000	100000	11000
Total bgd (W, Z, t,$t\bar{t}$)	156000	22000	101000	11500
$S/\sqrt{B}(W, Z, t, t\bar{t})$	2.9	2.8	2.4	2.5
$S/B(W, Z, t, t\bar{t})$	0.7%	1.9%	0.7%	2.3%

4.6. The QCD continuum background

The QCD continuum background has an initial cross-section which is several orders of magnitude higher than that for the other background processes (*e.g.* 10^6 times higher than Z+jet and 10^5 times higher than W+jet cross-sections). The inclusive production of the $b\bar{b}$ events themselves is of the order of 500 μb [1]. Missing energy in such events would mainly come from the mismeasured jets and from the limited acceptance of the detector. A quite significant fraction would come however also from the leptonic decays inside jets. For example, in the QCD $b\bar{b}$ events filtered on the $E_{\mathrm{T}}^{\mathrm{miss}} > 30$ GeV, around 38% of the events contain true missing energy $E_{\mathrm{T}}^{\nu} > 30$ GeV.

To suppress more efficiently the QCD background the additional selection criteria requiring isolation of the reconstructed transverse missing energy, $\Delta\phi(E_{\mathrm{T}}^{\mathrm{miss}}, \mathrm{jet}) > 0.5$, is used.

In the following, the QCD background and the ZH signal (as a control sample), are analysed with this additional selection requirement. For this analysis the selection criteria have been applied in different order than that in the analysis presented in the previous sections. It allows to study separately the acceptances for the jet- and lepton-veto and for the $E_{\mathrm{T}}^{\mathrm{miss}}$ isolation.

The acceptance of the initial selection criteria, as shown already in Table II, is 15.2% (with jet-veto) for ZH signal events with $Z \to \nu\nu$ and $H \to b\bar{b}$. It includes the efficiency of the event selection with $E_{\mathrm{T}}^{\mathrm{miss}} > 30$ GeV (77%), b-jets labelling (40%) and jet-veto (49%). In almost 100% of the cases the events have true missing energy, E_{T}^{ν}, above 30 GeV. For comparison with the QCD background discussed in the following, Table XIV shows the expected numbers of b-labelled signal events as a function of the $E_{\mathrm{T}}^{\mathrm{miss}}$ threshold. Specified are numbers of expected events after sequentially applied selection.

After additional selection criteria, as specified in Table XIV, and after applying b-tagging efficiency and acceptance in the mass window, around 238 events would be expected for the $E_{\mathrm{T}}^{\mathrm{miss}} > 30$ GeV threshold, see Table XX. If this threshold was raised to 50 GeV expected number of signal events would be reduced to 179.

TABLE XIV

The expected number of signal events ZH with $Z \to \nu\nu$ for an integrated luminosity of 30 fb^{-1} and inside the mass window $m_{bb} = 100 \pm 20$ GeV. b-tagging efficiency is not included.

Selection	$E_{\mathrm{T}}^{\mathrm{miss}} >$			
	30 GeV	35 GeV	40 GeV	50 GeV
2 b-labelled jets	1480	1382	1305	1133
$\Delta\phi(E_{\mathrm{T}}^{\mathrm{miss}}, j) > 0.5$	1244	1171	1111	983
Jet-veto	662	616	579	498
Lepton-veto	660	614	578	497

The contribution from the QCD background events was estimated from samples of the direct heavy flavour production, $gg, q\bar{q} \to b\bar{b}$, and from the QCD di-jet production. The sample of the $gg, q\bar{q} \to b\bar{b}$ was used as a control sample as it is giving a lower limit on the expected background. The $gg, q\bar{q} \to b\bar{b}$ production can be generated much more efficiently than the inclusive QCD $\to b\bar{b}$ background[3]. In fact, a consistency check was also performed for the $gg, q\bar{q} \to b\bar{b}$ contribution estimated from the inclusive QCD events and from a dedicated sample of the $gg, q\bar{q} \to b\bar{b}$ events. Initial cross-sections for these two samples are given in Table XV for each $p_{\mathrm{T}}^{\mathrm{hard}}$ bin. Tables XVI and XVII show the cumulative acceptances of the selection criteria for different types of QCD events.

Only events with $p_{\mathrm{T}}^{\mathrm{hard}} > 30$ GeV were analysed for both QCD $\to b\bar{b}$ and $gg, q\bar{q} \to b\bar{b}$. This was caused by the limited available CPU, given the extremely low acceptance for the inclusive QCD events generated in the lower range of $p_{\mathrm{T}}^{\mathrm{hard}}$. In the low $p_{\mathrm{T}}^{\mathrm{hard}}$ range, suppressing the cross-section for the QCD background to the level of the signal itself would require establishing a rejection of $\sim 10^{10}$. Such studies would therefore require simulating at least $\sim 10^{11}$ events. They have been nevertheless feasible for the $gg, q\bar{q} \to b\bar{b}$ sample where the required statistics was of 10^7 only. In fact, the contribution from the $p_{\mathrm{T}}^{\mathrm{hard}} = 10$–$30$ GeV range is found to be the dominant one for the total $gg, q\bar{q} \to b\bar{b}$ background. Table XVIII shows the expected number of events as a function of the successive selection and the different $E_{\mathrm{T}}^{\mathrm{miss}}$ thresholds, applied to the $gg, q\bar{q} \to b\bar{b}$ events generated in the $p_{\mathrm{T}}^{\mathrm{hard}} = 10$–$30$ GeV range.

Expected number of background events, estimated from samples generated with $p_{\mathrm{T}}^{\mathrm{hard}} > 30$ GeV for the inclusive QCD di-jet and for the $gg, q\bar{q} \to b\bar{b}$ processes, is given in Table XIX. For the final estimates on the number of expected events it was assumed that in the range $p_{\mathrm{T}}^{\mathrm{hard}} = 10$–$30$ GeV the direct $gg, q\bar{q} \to b\bar{b}$ production contributes 20% to the total QCD $\to b\bar{b}$ events (as it is in the case of the $p_{\mathrm{T}}^{\mathrm{hard}} > 30$ GeV range). The numbers obtained for the $gg, q\bar{q} \to b\bar{b}$ subsample were therefore rescaled accordingly. The acceptance of the 20–30% was estimated for the specified mass window, $m_{bb} = 100 \pm 20$ GeV.

The total QCD background is dominated by the true $b\bar{b}$ events. However, contribution from the direct heavy flavour production, $gg, q\bar{q} \to b\bar{b}$, is only on the level of 20% (this contribution is of 30% for the inclusive $b\bar{b}$ production). Around 1-3% of the selected events have true missing energy, E_{T}^{ν}, above 30 GeV.

[3] Here we mean inclusive QCD events where parton shower leads to the presence of the heavy quarks in the event.

TABLE XV

Production cross-sections for the QCD background processes.

	QCD $\to jj$ σ [pb]	$gg, q\bar{q} \to b\bar{b}$ σ [pb]
$p_{\mathrm{T}}^{\mathrm{hard}}$ = 10–30 GeV	5.9×10^9	1.7×10^7
$p_{\mathrm{T}}^{\mathrm{hard}}$ = 30–50 GeV	1.3×10^8	4.6×10^5
$p_{\mathrm{T}}^{\mathrm{hard}}$ = 50–100 GeV	2.1×10^7	8.0×10^4
$p_{\mathrm{T}}^{\mathrm{hard}}$ = 100–200 GeV	1.4×10^5	6.9×10^2
$p_{\mathrm{T}}^{\mathrm{hard}}$ => 200 GeV	7.4×10^4	2.6×10^2

TABLE XVI

For the different production processes, cumulative acceptances of the selection criteria (after initial selection). Question marks indicate that available statistics was not sufficient to give estimate on the acceptance.

Cumulative acceptance	$gg, q\bar{q} \to bb$	QCD $\to bb$	QCD $\to jb$	QCD $\to jj$
$E_{\mathrm{T}}^{\mathrm{miss}} > 30$ GeV				
2 labelled jets	100%	100%	100%	100%
$\Delta\phi(E_{\mathrm{T}}^{\mathrm{miss}}, j) > 0.5$	13.8%	21%	37%	70%
jet-veto	6.9%	7.6%	9.3%	–??–
lepton-veto	6.5%	7.0%	6.9%	–??–

TABLE XVII

For the different production processes, acceptances of the $E_{\mathrm{T}}^{\mathrm{miss}}$ threshold (after initial selection).

Acceptance	$gg, q\bar{q} \to bb$	QCD $\to bb$	QCD $\to jb$	QCD $\to jj$
$E_{\mathrm{T}}^{\mathrm{miss}} > 30$ GeV	100%	100%	100%	100%
$E_{\mathrm{T}}^{\mathrm{miss}} > 35$ GeV	48%	47%	47%	40%
$E_{\mathrm{T}}^{\mathrm{miss}} > 40$ GeV	25%	25%	23%	15%
$E_{\mathrm{T}}^{\mathrm{miss}} > 50$ GeV	7.5%	7.6%	6.3%	2.2%

TABLE XVIII

For an integrated luminosity of 30 fb^{-1}, the expected number of $gg, q\bar{q} \to b\bar{b}$ events from the sample generated with $p_T^{\rm hard}$ = 10–30 GeV. b-tagging efficiency and mass window acceptance are not included. In parenthesis given is fraction of events with the true missing energy $E_T^\nu > 30$ GeV. Indicated are also statistical errors of the given estimates.

Selection	$E_T^{\rm miss} >$			
	30 GeV	35 GeV	40 GeV	50 GeV
bb-lab. pair (10^6)	49 ± 1.9 ($9 \pm 1\%$)	18 ± 1.1 ($17 \pm 3\%$)	5.5 ± 0.7 ($25 \pm 6\%$)	0.4 ± 0.2 ($33 \pm 23\%$)
$\Delta\phi(E_T^{\rm miss}, j) > 0.5$ (10^6)	22 ± 1.3 ($0.3 \pm 2.5\%$)	8.2 ± 0.8 ($14.5 \pm 1.5\%$)	2.8 ± 0.4 ($4.9 \pm 0.9\%$)	0.22 ± 0.13 (–??–)
jet-veto (10^6)	19 ± 1.2 ($39 \pm 2.5\%$)	7.1 ± 0.7 ($14.5 \pm 1.5\%$)	2.4 ± 0.4 ($4.9 \pm 0.9\%$)	0.15 ± 0.1 (–??–)
lepton-veto (10^6)	15 ± 1.0 ($30 \pm 2\%$)	5.6 ± 0.6 ($1 \pm 1\%$)	1.8 ± 0.4 (–??–)	0.15 ± 0.1 (–??–)

From the study presented above the following estimates on the expected backgrounds can be extracted, including acceptance inside mass window and nominal b-tagging efficiency, for the selection threshold $E_T^{\rm miss}$ > 35 GeV:

- The contribution from the $gg, q\bar{q} \to b\bar{b}$ hard process resulting with 2 b-tagged jets in the final state is $(0.7 \pm 0.05) \times 10^6$ events. Note that contributions listed in Tables XVIII and XIX have been added. At most few percent of them have true $E_T^\nu > 30$ GeV.

- The total QCD di-jet contribution from $gg, gq, q\bar{q} \to q\bar{q}, gg, gq$ processes to the background events with two b-labelled jets in the final state (from hard process or parton shower) is much higher. On the production level is higher only by factor 3, however after selection, as specified above, is higher by factor 5, see Table XIX. This ratio was estimated from events generated with $p_T^{\rm hard} > 30$ GeV and such estimate might be a bit pessimistic. In total, about $(3.8 \pm 0.5) \times 10^6$ background events are expected after all cuts with 1% of them having E_T^ν above 30 GeV. The QCD background is steeply falling with raising threshold on the $E_T^{\rm miss}$. It is reduced by factor 30 if this threshold is raised to 50 GeV.

TABLE XIX

For an integrated luminosity of 30 fb^{-1}, the expected number of the inclusive QCD events and the $gg \to b\bar{b}$ events, both generated with $p_{\mathrm{T}}^{\mathrm{hard}} > 30$ GeV. The b-tagging efficiency and mass window acceptance is not included. In parenthesis given is the fraction of events with true missing energy $E_{\mathrm{T}}^{\nu} > 30$ GeV. Indicated are also statistical errors of the given estimates.

Selection	$E_{\mathrm{T}}^{\mathrm{miss}} >$ 30 GeV	35 GeV	40 GeV	50 GeV
	Units are 10^6			
	$gg, q\bar{q} \to b\bar{b}$			
bb-lab. pair	81 ± 0.1 (38%)	39 ± 0.1 (58%)	20 ± 0.06 (74%)	6.0 ± 0.02 (91%)
$\Delta\phi(E_{\mathrm{T}}^{\mathrm{miss}}, j) > 0.5$	11 ± 0.07 (5.8 ± 0.1%)	4.2 ± 0.04 (9.9 ± 0.2%)	1.7 ± 0.03 (14.8 ± 0.4%)	0.26 ± 0.01 (28 ± 1%)
jet-veto	5.5 ± 0.06 (2.1 ± 0.1%)	2.2 ± 0.04 (3.7 ± 0.05%)	0.8 ± 0.02 (5.7 ± 0.3%)	0.13 ± 0.008 (12 ± 1.2%)
lepton-veto	5.3 ± 0.06 (1.9 ± 0.1%)	2.0 ± 0.04 (3.1 ± 0.2%)	0.8 ± 0.02 (4.5 ± 0.3%)	0.12 ± 0.007 (8.7 ± 1.0%)
	QCD $\to b\bar{b}$			
bb-lab. pair	380 ± 7.3 (33%)	180 ± 4.2 (51%)	97 ± 3.0 (65%)	29 ± 0.8 (85%)
$\Delta\phi(E_{\mathrm{T}}^{\mathrm{miss}}, j) > 0.5$	82 ± 4.9 (4.3 ± 0.5%)	36 ± 3.1 (5.8 ± 0.7%)	16 ± 2.2 (7.3 ± 1.1%)	2.3 ± 0.5 (15 ± 3%)
jet-veto	29 ± 3.4 (1.2 ± 2.7%)	13 ± 2.2 (6.8 ± 6.4%)	6.6 ± 1.6 (14 ± 13%)	1.4 ± 0.5 (50 ± 50%)
lepton-veto	27 ± 3.4 (–??–)	11 ± 2.2 (–??–)	5.5 ± 1.5 (–??–)	0.6 ± 0.2 (–??–)
	QCD $\to jb$			
jb-lab. pair	1100 ± 13 (21%)	500 ± 7.8 (34%)	230 ± 4.4 (48%)	60 ± 2 (71%)
$\Delta\phi(E_{\mathrm{T}}^{\mathrm{miss}}, j) > 0.5$	400 ± 10 (4.0 ± 0.2%)	180 ± 6.6 (7.0 ± 0.5%)	70 ± 3.6 (13 ± 1%)	12 ± 1.7 (35 ± 5%)

- The QCD di-jet contribution to the events with jb-labelled pair, after all selection criteria, is almost a factor of 3 higher than those to the events with bb-labelled pair. If the b-tagging efficiency is taken into account (with a non-b jet rejection of 100) and 20–30% acceptance in the mass window is assumed, the expected background would be below 10^5 events.
- The QCD di-jet contribution to the events with jj-labelled pairs is on the level of 100 ± 30 events at most, just being negligible for jet rejection efficiency of 100. This estimate is obtained before applying jet-veto and lepton-veto cuts.

The QCD background is overwhelming for the $E_{\rm T}^{\rm miss} + b\bar{b}$ signature. For the $E_{\rm T}^{\rm miss}$ threshold of 30 GeV it is a factor of 5×10^2 higher than the total background from W and Z. Final estimates for the ZH signal and QCD background rates are given in Table XX.

TABLE XX

For an integrated luminosity of 30 fb^{-1}, the expected number of ZH signal and QCD bb and jb background events. The b-tagging efficiency and mass window acceptance are included.

Selection	$E_{\rm T}^{\rm miss} >$			
	30 GeV	35 GeV	40 GeV	50 GeV
ZH Signal	238	221	208	179
QCD $\to b\bar{b}$	$(10 \pm 1.0) \times 10^6$	$(3.8 \pm 0.5) \times 10^6$	$(1.6 \pm 0.3) \times 10^6$	$(0.12 \pm 0.05) \times 10^6$
QCD $\to jb$	$< 10^5$	$< 10^5$	$< 10^5$	$< 10^5$
S/B	0.003%	0.007%	0.02%	0.14%
$S/\sqrt{B}$	0.07	0.13	0.21	0.50

4.7. Conclusions

A detailed analysis of the accessibility of the WH/ZH channels with the $E_{\rm T}^{\rm miss} + b\bar{b}$ final state signature has been discussed for the 14 TeV pp collision. If only background processes with the W and Z in the final state were considered, significance of at most 3σ could be expected for an integrated luminosity of 30 fb^{-1}. The background to this signature would be dominated by the true $Zb\bar{b}$ events.

However in the presence of the huge QCD background this channel becomes hopeless. Even with the optimised selection criteria and with rising missing threshold on the transverse energy *e.g.* to $E_{\rm T}^{\rm miss} > 50$ GeV, the expected signal-to-background ratio is below 0.15% and the expected sensitivity remains below 1σ for an integrated luminosity of 30 fb^{-1}. Those numbers are by far very optimistic as the fast simulation, used to simulate detector performance, represents the very crude approach for the reducible backgrounds with the $E_{\rm T}^{\rm miss}$ signature. In addition the feasibility and efficiency for triggering on such events was not discussed here.

5. 2 TeV $p\bar{p}$ versus 14 TeV pp

The WH/ZH channel with $E_{\rm T}^{\rm miss} + b\bar{b}$ signature is considered as having discovery potential at Tevatron [2]. The quantitative comparison of the expected rates have been performed assuming comparable performance of the detectors at both colliders, namely efficiencies for jets and lepton reconstruction, b-jet tagging, jet veto and $E_{\rm T}^{\rm miss}$ resolution.

For the presented below comparison consistently the following selection criteria were used:

- Relatively low missing transverse energy threshold $E_{\mathrm{T}}^{\mathrm{miss}} > 30$ GeV.
- For the cases called (1) and (2), kinematical coverage of the ATLAS detector and selection criteria as discussed in previous Section. Differences in acceptances and expected rates are therefore directly related to differences in the cross-sections and geometrical features of events (*eg.* events at 2 TeV are more central than at 14 TeV).
- For the case called (3) reduced geometrical coverage and slightly different selection criteria, as specified in the Tevatron report [2].
  - b-tagging and isolated lepton coverage up to $\eta < 2.0$;
  - lepton-veto: veto lepton with $p_{\mathrm{T}} > 10$ GeV;
  - jet-veto: coverage up to $|\eta| < 2.5$; no jets $p_{\mathrm{T}} > 30$ GeV, no more than one jet[4] with $p_{\mathrm{T}} > 15$ GeV.
- For b-tagging efficiency the 60% efficiency per b-labelled jet, with rejection 10 per c-jet and 100 per light jet.
- The mass window of 100 ± 20 GeV, leading to the signal acceptance in the mass window of 85%.

For comparison of the expected signal and background rates at the 14 TeV pp and 2 TeV $p\bar{p}$ we refer to the cases (1) and (3). These already take into account differences in the geometrical acceptances of the detectors at respective colliders and optimisation of the selection criteria.

5.1. ZH and WH signals

The effective acceptance for signal events is higher for 2 TeV $p\bar{p}$ scenario (3) than for 14 TeV scenario (1). Acceptance for the $E_{\mathrm{T}}^{\mathrm{miss}}$ and lepton veto is comparable except the WH, $W \to \ell\nu$ channel where it is higher by factor 2.6 for the 14 TeV pp. Final acceptance after jet-veto is higher in the 2 TeV scenario; by factor 2 for $Z \to \nu\nu$ and $W \to \ell\nu$ channels and by factor 3 for $Z \to \tau\tau$ and $W \to \tau\nu$ channels. This factor 3 is mostly due to the softer jet-veto applied to hadronic decays of the tau leptons in the case (3).

[4] This threshold is set on the reconstructed jets energies [3]. It corresponds to 10 GeV threshold on 100% efficient calorimetric reconstruction in cone $\Delta R = 0.4$ and 15 GeV threshold after applying Gaussian smearing with $50\%/\sqrt{E}$ resolution [11]. It is equivalent to 22 GeV threshold on recalibrated jet energies.

TABLE XXI

For the ZH and WH signal events, cumulative acceptances of the selection criteria. b-tagging efficiency and acceptances in the mass window are not included.

Cumulative acceptance	14 TeV pp (1)	2 TeV $p\bar{p}$ (2)	2 TeV $p\bar{p}$ (reduced) (3)	Ratio (1)/(3)
	ZH, $Z \to \nu\nu$			
$E_{\mathrm{T}}^{\mathrm{miss}}$+lepton veto	77.3%	73.2%	73.4%	1.0
+ 2 b-labelled jets	31.2%	39.6%	37.6%	0.8
+ jet veto	15.2%	27.0%	31.0%	0.5
	ZH, $Z \to \tau\tau$			
$E_{\mathrm{T}}^{\mathrm{miss}}$+lepton veto	26.3%	19.0%	19.6%	1.3
+ 2 b-labelled jets	9.3%	10.2%	9.9%	0.9
+ jet veto	0.8%	1.3%	3.0%	0.3
	WH, $W \to \tau\nu$			
$E_{\mathrm{T}}^{\mathrm{miss}}$+lepton veto	52.3%	45.8%	46.4%	1.1
+ 2 b-labelled jets	19.8%	24.9%	24.0%	0.8
+ jet veto	4.2%	8.1%	13.4%	0.3
	WH, $W \to \ell\nu$			
$E_{\mathrm{T}}^{\mathrm{miss}}$+lepton veto	16.3%	4.9%	6.2%	2.6
+ 2 b-labelled jets	4.0%	2.6%	3.0%	1.3
+ jet veto	1.2%	1.5%	2.4%	0.5

TABLE XXII

For an integrated luminosity of 30 fb^{-1}, expected number of events from the ZH and WH signal after all cuts including jet-veto. Numbers are given including nominal b-tagging efficiency and acceptance inside mass window.

Expected events	14 TeV pp (1)	2 TeV $p\bar{p}$ (2)	2 TeV $p\bar{p}$ (reduced) (3)	Ratio (1)/(3)
ZH with $Z \to \nu\nu$	293	57	65	4.2
ZH with $Z \to \tau\tau$	3	1	1	3.0
WH with $W \to \tau\nu$	77	16	26	3.0
WH with $W \to \ell\nu$	44	6	9	4.9
Total signal	417	80	101	4.1

After complete selection and after adding all signal contributions together the total signal rate is higher by factor 4 in the 14 TeV scenario.

5.2. ZZ and WZ resonant background

Similarly as for the signal events, the effective acceptance for these resonant backgrounds is higher by factor 2 for $Z \to \nu\nu$, $W \to \ell\nu$ and factor 3 for $Z \to \tau\tau$ and $W \to \tau\nu$ channels in the 2 TeV scenario. Taking into account ratio of the initial cross-sections, rates for these backgrounds are larger by factor 5 in the 14 TeV scenario. As the signal rates are larger by factor 4, the signal-to-resonant-background ratio is only slightly worse in the 14 TeV scenario.

TABLE XXIII

The same as Table XXI but for the ZZ and WZ events.

Cumulative acceptance	14 TeV pp (1)	2 TeV $p\bar{p}$ (2)	2 TeV $p\bar{p}$ (reduced) (3)	Ratio (1)/(3)
	ZZ, $Z \to \nu\nu$			
$E_{\mathrm{T}}^{\mathrm{miss}}$+lepton veto	68.5%	64.2%	64.5%	1.0
+ 2 b-labelled jets	24.5%	29.5%	27.5%	0.9
+ jet veto	12.0%	20.7%	23.1%	0.5
	ZZ, $Z \to \tau\tau$			
$E_{\mathrm{T}}^{\mathrm{miss}}$+lepton veto	20.7%	14.0%	14.6%	1.4
+ 2 b-labelled jets	6.8%	6.5%	6.4%	1.1
+ jet veto	0.7%	1.1%	2.2%	0.3
	WZ, $W \to \tau\nu$			
$E_{\mathrm{T}}^{\mathrm{miss}}$+lepton veto	49.7%	43.1%	44.1%	1.1
+ 2 b-labelled jets	16.5%	19.0%	17.4%	0.9
+ jet veto	3.9%	6.9%	10.8%	0.4
	WZ, $W \to \ell\nu$			
$E_{\mathrm{T}}^{\mathrm{miss}}$+lepton veto	17.9%	4.4%	8.7%	2.0
+ 2 b-labelled jets	5.8%	2.1%	3.5%	1.6
+ jet veto	1.8%	1.2%	2.9%	0.6

TABLE XXIV

The same as Table XXII but for the ZZ and WZ events.

Expected events	14 TeV pp (1)	2 TeV $p\bar{p}$ (2)	2 TeV $p\bar{p}$ (reduced) (3)	Ratio (1)/(3)
ZZ with $Z \to \nu\nu$	670	100	112	6.0
ZZ with $Z \to \tau\tau$	10	1	3	2.7
WZ with $W \to \tau\nu$	135	21	35	3.8
WZ with $W \to \ell\nu$	125	8	20	6.2
Total res. bgd	940	130	170	5.5

5.3. Zjj and Wjj continuum background

The Zjj with $Z \to \nu\nu$ and Wjj with $W \to \ell\nu$ events were simulated with PYTHIA. Contribution from events with the $Z \to \tau\tau$ decay is negligible and for simplicity was omitted. Contribution from the $W \to \tau\nu$ events was estimated assuming the same ratio of acceptances as for the WZ events with $W \to \tau\nu$ and $W \to \ell\nu$.

Contribution from the Zbb events is a dominant one, almost 90% of the total Zjj background. Expected rates in the mass window are higher by factor almost 30 with 14 TeV scenario. This is comparable to the ratio of rates expected for the $\ell\ell b\bar{b}$ final state [3]. Contribution from the Wbb events is less dominant, around 40% of the total Wjj background for the 2 TeV $p\bar{p}$ and around 70% for the 14 TeV pp. Also expected ratio of rates is higher with the 14 TeV scenario, being for the $W \to \ell\nu$ events almost 20.

TABLE XXV

The same as Table XXI but for Zjj events ($Z \to \nu\nu$) for events already filtered on 2 jets within $|\eta| < 2.5$. Acceptances are given for merged samples generated in different bins of $p_{\mathrm{T}}^{\mathrm{hard}}$.

Cumulative acceptance	14 TeV pp (1)	2 TeV $p\bar{p}$ (2)	2 TeV $p\bar{p}$ (reduced) (3)	Ratio (1)/(3)
$E_{\mathrm{T}}^{\mathrm{miss}}$+lepton veto	82.2%	92.4 %	92.4%	0.9
+ 2 jets $|\eta| < 2.0$ (2.5)	filter	filter	filter	—
+ jet veto	23.9%	42.1%	48.5%	0.5

TABLE XXVI

The same as Table XXI but for Wjj with $W \to \ell\nu$ evets.

Cumulative acceptance	14 TeV pp (1)	2 TeV $p\bar{p}$ (2)	2 TeV $p\bar{p}$ (reduced) (3)	Ratio (1)/(3)
$E_{\rm T}^{\rm miss}$+lepton veto	17.2 %	6.0%	8.3%	2.1
+ 2 jets η < 2.0 (2.5)	11.2%	5.2%	7.0%	1.6
+ jet veto	3.0%	3.1%	6.0%	0.5

TABLE XXVII

The same as Table XXII but for Zjj and Wjj events.

Expected events	14 TeV pp (1)	2 TeV $p\bar{p}$ (2)	2 TeV $p\bar{p}$ (reduced) (3)	Ratio (1)/(3)
	Zjj			
(bb)	14000	450	520	27
(other)	1800	40	50	36
	Wjj			
(bb)	3100	80	180	21
(other)	1300	50	80	16

5.4. Top pair and single top background

• **$t\bar{t}$ continuum background**

The $t\bar{t}$ background, substantial for the $\ell b\bar{b}$ final state signature is less severe in the case of the $E_{\rm T}^{\rm miss} + b\bar{b}$ final state. With rather tight jet-veto foreseen in 14 TeV scenario, effective acceptance is 10 times lower for the $W \to \tau\nu$ decays and 5 times lower for the $W \to \ell\nu$ decays. Effectively, this background is only 15 times higher in 14 TeV scenario, nevertheless contributing only few percent to the total background.

• **Single top continuum background**

The single top background, rather small for $\ell b\bar{b}$ final state signature, is also small in the case of $E_{\rm T}^{\rm miss} + b\bar{b}$ final state. With rather tight jet-veto foreseen in 14 TeV scenario effective acceptance is 3 times lower for $W \to \tau\nu$ decays and 5 times lower for $W \to \ell\nu$ decays. Effectively, this background is only 8 times higher in the 14 TeV scenario and is contributing below one percent to the total background.

TABLE XXVIII

The same as Table XXI but for $t\bar{t}$ events.

Cumulative acceptance	14 TeV pp (1)	2 TeV $p\bar{p}$ (2)	2 TeV $p\bar{p}$ (reduced) (3)	Ratio (1)/(3)
	$t\bar{t}$ with at least one $W \to \tau\nu$			
$E_{\rm T}^{\rm miss}$+lepton veto	47.9%	43.4%	44.4%	1.1
+ 2 b-labelled jets	27.0%	27.8%	27.3%	1.0
+ jet veto	0.16%	0.3%	1.2%	0.1
	$t\bar{t}$ with at least one $W \to \ell\nu$			
$E_{\rm T}^{\rm miss}$+lepton veto	12.4%	6.4%	8.7%	1.4
+ 2 b-labelled jets	6.5%	4.2%	5.5%	1.2
+ jet veto	0.09%	0.1%	0.4%	0.2

TABLE XXIX

The same as Table XXI but for single top events already filtered on at least 2 b- or c-labelled jets.

Cumulative acceptance	14 TeV pp (1)	2 TeV $p\bar{p}$ (2)	2 TeV $p\bar{p}$ (reduced) (3)	Ratio (1)/(3)
	Single top with $W \to \tau\nu$			
$E_{\rm T}^{\rm miss}$+lepton veto	57.7%	51.7%	50.9%	1.1
+ 2 b-labelled jets	27.1%	20.7%	24.9%	1.1
+ jet veto	0.4%	0.35%	1.3%	0.3
	Single top with $W \to \ell\nu$			
$E_{\rm T}^{\rm miss}$+lepton veto	11.2%	5.4%	7.9%	1.4
+ 2 b-labelled jets	5.8%	3.2%	4.0%	1.4
+ jet veto	0.15%	0.3%	0.8%	0.2

- **$W^* \to tb$ continuum background**

This background, similarly as for the $\ell b\bar{b}$ signature, is rather small. Only the $W \to \ell\nu$ decay mode could be simulated with available version of the HERWIG Monte Carlo. It was therefore assumed that this channel behaves similarly to the tb, tc single production, see Table XXIX, so that the acceptance before jet veto is 6.2 higher and after jet-veto is 1.6 higher for the $W \to \tau\nu$ than for the $W \to \ell\nu$ final state.

With rather tight jet-veto foreseen in 14 TeV scenario cumulative acceptance is 2.5 times lower. Effectively, this background is only 6 times higher in 14 TeV scenario nevertheless contributing only few percent to the total background.

TABLE XXX

The same as Table XXI but for $W^* \to tb$ events with $W \to \ell\nu$ decay.

Cumulative acceptance	14 TeV pp (1)	2 TeV $p\bar{p}$ (2)	2 TeV $p\bar{p}$ (reduced) (3)	Ratio (1)/(3)
$E_{\rm T}^{\rm miss}$+lepton veto	19.0%	5.4%	9.1%	2.1
+ 2 b-labelled jets	7.4%	4.0%	6.3%	1.2
+ jet veto	2.0%	2.0%	4.7%	0.4

- **Total continuum background from top events**

TABLE XXXI

The same as Table XXII but for single and top pair production.

Expected events	14TeV pp (1)	2 TeV $p\bar{p}$ (2)	2 TeV $p\bar{p}$ (reduced) (3)	Ratio (1)/(3)
	$t\bar{t}$			
With $W \to \tau\nu$	340	5	20	17
With $W \to \ell\nu$	440	4	30	15
	$W^* \to tb$			
Total	90	15	40	6
	Single top $tb,\ tc$			
Total	50	2	6	8

5.5. Total signal and W, Z, single top and top-pair backgrounds

Table XXXII compares expected signal and background rates in 14 TeV pp and 2 TeV $p\bar{p}$ collisions for selection with jet-veto. The expected signal is higher by factor 4 and background by factor 20 in 14 TeV scenario.

TABLE XXXII

For an integrated luminosity of 30 fb^{-1}, expected number of signal and background events after all cuts. Acceptance inside mass window and nominal b-tagging efficiency are included.

Process	14 TeV pp (1)	2 TeV $p\bar{p}$ (2)	2 TeV $p\bar{p}$ (reduced) (3)	Ratio (1)/(3)
ZH	296	58	66	4.5
WH	121	22	35	3.4
Total signal	417	80	101	4.1
ZZ	680	101	115	5.9
WZ	260	29	55	4.7
Total reson. bgd	940	130	170	5.5
tt	780	9	50	16
single t	140	17	46	3.0
Zjj (bb)	14000	450	520	27
Zjj (other)	1800	40	50	36
Wjj (bb)	3100	80	180	20
Wjj (other)	1300	50	80	16
Total cont. bgd (W, Z, t,$t\bar{t}$)	21000	650	900	23
Total bgd (W, Z, t,$t\bar{t}$)	22000	800	1100	20
$S/\sqrt{B}$ (W, Z, t,$t\bar{t}$)	2.8	2.8	3.0	0.9
S/B (W, Z, t,$t\bar{t}$)	1.9%	10.0%	9.2%	0.2

Taking into account only physics background (W, Z, t, $t\bar{t}$ in the final state), sensitivity to this channel in terms of $S/\sqrt{B}$ is comparable for 14 TeV pp and 2 TeV $p\bar{p}$, being of 3 σ for an integrated luminosity 30 fb^{-1}.

However, the overwhelming QCD background in both cases reduces this sensitivity significantly. In the case of 14 TeV scenario is reduced below 1 σ. As discussed already in Section 4.6, applied so far selection can be optimised further to stronger suppress QCD background, while still keeping high signal efficiency. This additional suppression would have to be of factor $5{\cdot}10^3$ in the 14 TeV scenario, which is not achieved in the presented analysis, to bring the QCD background below 10% of the backgrounds with true missing energy from W and Z decays. In the next Section this background is evaluated for the 2 TeV scenario.

5.6. The QCD continuum background

In this Section more detailed discussion is presented on the evaluation of the QCD background at 2 TeV $p\bar{p}$, obtained from the simulation with PYTHIA Monte Carlo.

The evaluation is done only for events with $p_{\mathrm{T}}^{\mathrm{hard}} > 30$ GeV. As can be concluded from numbers in Section 4.6, it might significantly underestimate the level of the total background as the contribution from events with $p_{\mathrm{T}}^{\mathrm{hard}} < 30$ GeV is rather important. In that range however available statistics was by far no sufficient for reliable estimate of the background contribution.

For the presented below evaluation the following selection criteria were used:

- $E_{\mathrm{T}}^{\mathrm{miss}}$ calculated from reconstructed energy with calorimetric coverage up to $|\eta| < 5.0$.
- $\Delta\phi(E_{\mathrm{T}}^{\mathrm{miss}}, \mathrm{jet}) > 0.5$.
- Two b-tagged jets in rapidity up to $|\eta| < 2.0$; Jets reconstruction threshold was set to 15 GeV and jets energies were recalibrated.
- Jet-veto: coverage up to $|\eta| < 2.5$; no jets $p_{\mathrm{T}} > 30$ GeV, no more than one jet $p_{\mathrm{T}} > 15$ GeV.
- Lepton veto: isolated lepton with and $|\eta| < 2.0$ and $p_{\mathrm{T}} > 10$ GeV.
- Additional selection[5]: $\Delta\phi(E_{\mathrm{T}}^{\mathrm{miss}}, \mathrm{jet}) > 1.0$ and $\Delta\phi(\mathrm{jet}_1, \mathrm{jet}_2) < 2.6$
- For b-tagging efficiency the 60% efficiency per b-labelled jet, with rejection 10 per c-jet and 100 per light jet.
- The mass window of 100 ± 20 GeV.

[5] These were suggested by W. Yao as a refinement to selection documented in [2], private communication.

The acceptance of the initial selection criteria is 38% for signal events ZH with $Z \to \nu\nu$. It requires passing selection of having $E_{\rm T}^{\rm miss} > 30$ GeV (80%) and 2 b-labelled jets (48%). The acceptance of 85% is assumed inside mass window of $m_{bb} = 100 \pm 20$ GeV. In almost 100% of cases, events have true missing energy $E_{\rm T}^{\nu} > 30$ GeV.

After additional selection criteria, as specified in Table XXXIII, around 135 events would be expected for an integrated luminosity of 30 fb^{-1} with perfect b-tagging and the threshold $E_{\rm T}^{\rm miss} > 35$ GeV. After applying b-tagging efficiency this number would be reduced to 50 events, see Table XXXVIII. If the threshold was raised to 50 GeV it would be reduced further to 40 expected events.

TABLE XXXIII

For an integrated luminosity of 30 fb^{-1}, the expected number of signal ZH events in 2 TeV $p\bar{p}$ collision (mass window $m_{bb} = 100 \pm 20$ GeV). b-tagging efficiency is not included.

Selection	$E_{\rm T}^{\rm miss} >$			
	30 GeV	35 GeV	40 GeV	50 GeV
bb-lab. pair	223	205	188	155
$\Delta\phi(E_{\rm T}^{\rm miss}, j) > 0.5$	197	183	169	141
jet-veto	167	154	142	118
lepton-veto	167	154	141	117
additional cuts	143	135	126	108

Contribution from the QCD events was estimated from the samples of the direct $b\bar{b}$ production, $gg, q\bar{q} \to b\bar{b}$, and from the QCD di-jet production. The sample of $gg, q\bar{q} \to b\bar{b}$ was used as a control sample.

In Table XXXIV initial cross-section is compared for each $p_{\rm T}^{\rm hard}$ bin. The efficiency for filter is also specified (events were filtered on $E_{\rm T}^{\rm miss} > 30$ GeV and 2 jets with $|\eta| < 2.5$). Altogether, for presented below analysis, 10^8 events have been proceeded through the fast simulation of the ATLAS detector.

Tables XXXV–XXXVII give details on the cumulative acceptances for the QCD background. Table XXXVIII specifies expected number of events for an integrated luminosity of 30 fb^{-1} and for different thresholds on the transverse missing energy. The set of distributions, which are relevant for the selection algorithm, are presented in Figs. 1–4 for signal and different types of QCD background.

From the study presented above the following estimates on the expected backgrounds can be extracted for 35 GeV threshold on $E_{\rm T}^{\rm miss}$, including ac-

TABLE XXXIV

Production cross-sections and filter acceptance, see text, for QCD background processes for 2 TeV $p\bar{p}$ and filter efficiency. For the case of $p_{\rm T}^{\rm hard}$ = 30–50 GeV (resp. 50–100 GeV) average acceptance is given for events generated in 5 GeV (resp. 10 GeV) bins.

	QCD jets		$gg, q\bar{q} \to b\bar{b}$	
Hard scattering transverse momenta	σ [pb]	Filter accept.	σ [pb]	Filter accept.
$p_{\rm T}^{\rm hard}$ = 10–30 GeV	5.0×10^8		1.4×10^6	
$p_{\rm T}^{\rm hard}$ = 30–50 GeV	1.0×10^6	0.14%	1.9×10^5	0.3%
$p_{\rm T}^{\rm hard}$ = 50–100 GeV	5.8×10^5	0.33%	2.1×10^3	4.4%
$p_{\rm T}^{\rm hard}$ = 100–200 GeV	1.7×10^4	1.0%	7.7×10^0	21%
$p_{\rm T}^{\rm hard}$ => 200 GeV	2.2×10^2	3.6%	2.0×10^0	30%

TABLE XXXV

For indicated production processes and 2 TeV $p\bar{p}$ scenario, cumulative acceptances of the selection criteria.

Cumulative acceptance	$gg, q\bar{q} \to bb$	QCD $\to bb$	QCD $\to jb$	QCD $\to jj$
$E_{\rm T}^{\rm miss}$ > 30 GeV				
2 labelled jets	100%	100%	100%	100%
$\Delta\phi(E_{\rm T}^{\rm miss}, j) > 0.5$	2.5%	10%	32%	71%
jet-veto	2.0%	6%	9%	– ?? –
lepton-veto	1.5%	4%	6%	– ?? –
additional cuts	0.7%	2%	4%	– ?? –

ceptance inside mass window and nominal b-tagging efficiency. This background might be still underestimated as only events with $p_{\rm T}^{\rm hard}$ > 30 GeV were analysed.

- Contribution from $gg, q\bar{q} \to b\bar{b}$ events, is of 1152 ± 76 events with 8% of them having true $E_{\rm T}^{\nu}$ > 30 GeV.
- The total QCD di-jet contribution to the events with 2 true b-labelled jets is almost factor 4 higher. About 4500 ± 800 events are expected with (18 ± 11)% of events having $E_{\rm T}^{\nu}$ above 30 GeV. The QCD background is steeply falling down with raising the threshold on the $E_{\rm T}^{\rm miss}$.

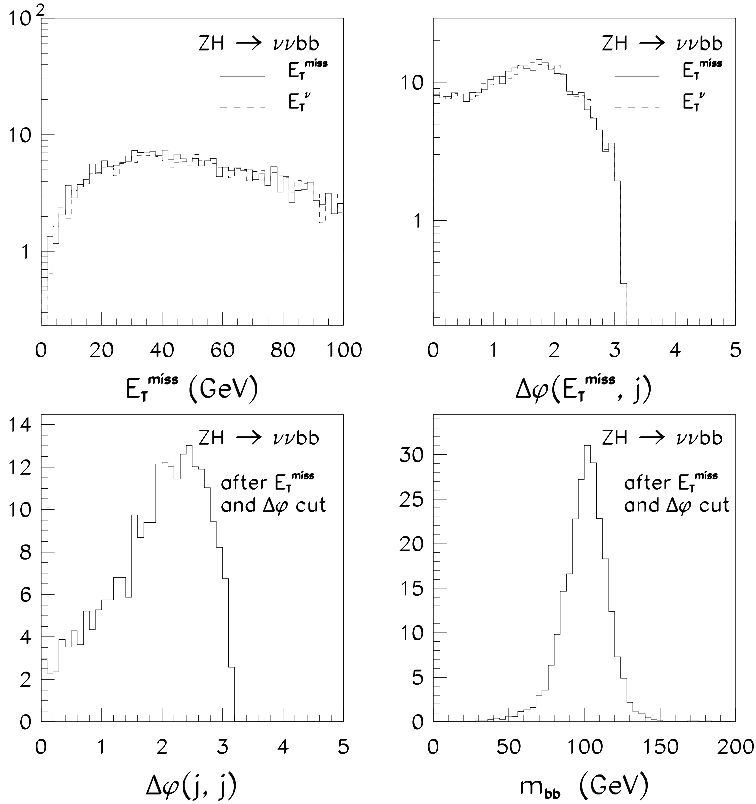

Fig. 1. The $E_{\rm T}^{\rm miss}$, $\Delta\phi(E_{\rm T}^{\rm miss}, {\rm jet})$, $\Delta\phi$ (jet, jet) and m_{bb} distributions for events after initial selection. Dashed lines on top plots show corresponding $E_{\rm T}^{\nu}$ and $\Delta\phi(E_{\rm T}^{\nu}$, jet) distribution. The $\Delta\phi$ (jet, jet) and m_{bb} distributions are shown for events after selection on $E_{\rm T}^{\rm miss} > 30$ GeV and $\Delta\phi(E_{\rm T}^{\nu}, {\rm jet}) > 0.5$.

TABLE XXXVI

For indicated production processes and 2 TeV $p\bar{p}$, acceptances of the $E_{\rm T}^{\rm miss}$ thresholds (after initial filter).

Cumulative acceptance	$gg \to bb$	QCD $\to bb$	QCD $\to jb$	QCD $\to jj$
$E_{\rm T}^{\rm miss} > 30$ GeV	100%	100%	100%	100%
$E_{\rm T}^{\rm miss} > 35$ GeV	44%	50%	45%	34%
$E_{\rm T}^{\rm miss} > 40$ GeV	20%	24%	21%	12%
$E_{\rm T}^{\rm miss} > 50$ GeV	5%	8%	6%	1.7%

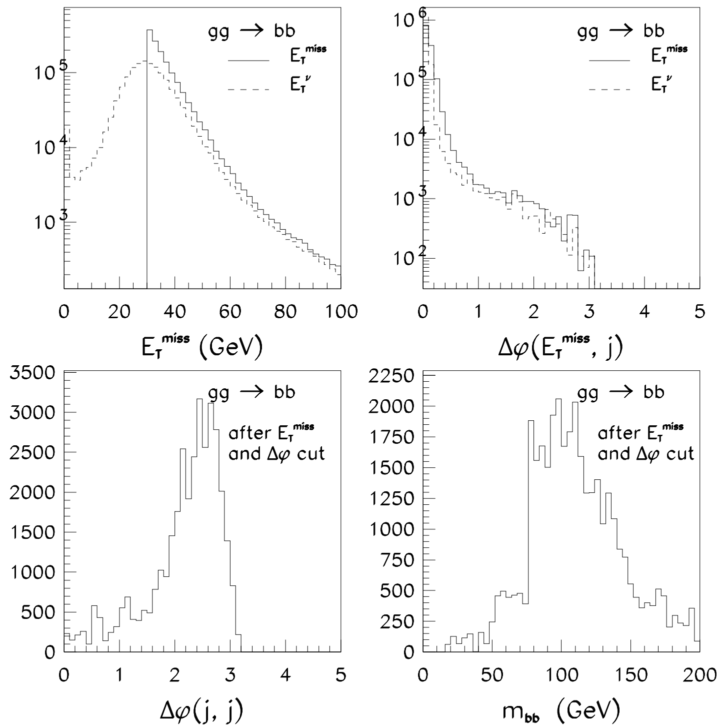

Fig. 2. The same as Fig 1 but for $gg \to b\bar{b}$ events. The $E_{\rm T}^{\rm miss}$ and $\Delta\phi(E_{\rm T}^{\nu}$, jet) distributions are shown for events filtered on $E_{\rm T}^{\rm miss} > 30$ GeV and 2 jets with $|\eta| < 2.5$. The $\Delta\phi$ (jet, jet) and m_{bb} distributions are shown after further selection on $\Delta\phi(E_{\rm T}^{\nu}, {\rm jet}) > 0.5$.

It is reduced almost by factor 10 if this threshold is raised to 50 GeV, containing however $97 \pm 66\%$ of events with true missing energy above 30 GeV.

- The QCD di-jet contribution to the events with jb-labelled pair is factor 5 higher than these to bb-labelled pairs. The expected background would be of 350 ± 50 events, with non-b jets rejection of 100. This might be a bit optimistic estimate since some of these events contain also bc-labelled pairs (for c-labelled jets expected rejection is only 10).

- The QCD di-jet contribution to the events with jj-labelled pairs is on the level of 500 ± 100 events at most. This estimate is done before applying jet-veto and lepton-veto.

The total QCD background is dominated by the true QCD $\to b\bar{b}$ events. However, contribution from the direct heavy flavour production $gg, q\bar{q} \to b\bar{b}$

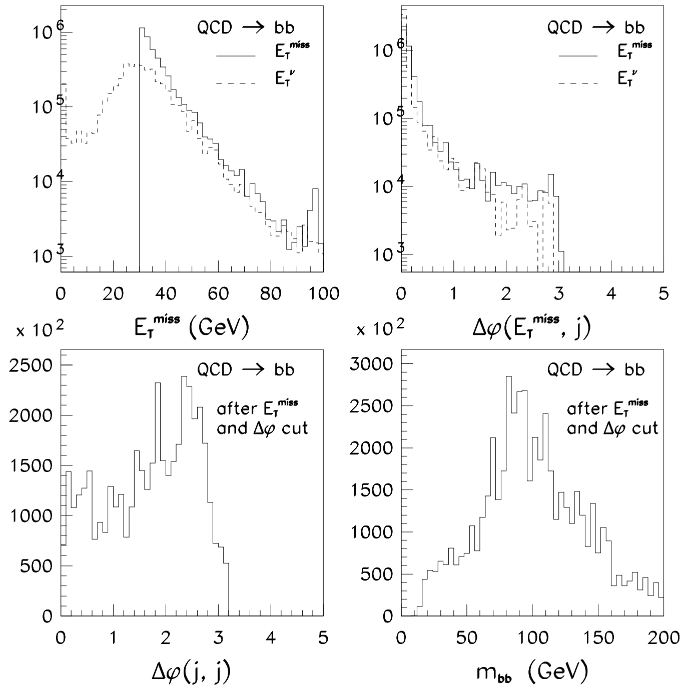

Fig. 3. The same as Fig 2 but for QCD $\rightarrow b\bar{b}$ events.

is only on the level of 25% (this contribution is of 30% for inclusive $b\bar{b}$ production). Around 20% of QCD events have true missing energy, E_{T}^{ν}, above 30 GeV.

The QCD background is steeply falling with $E_{\mathrm{T}}^{\mathrm{miss}}$ selection. Raising threshold from 30 GeV to 50 GeV reduces $gg, q\bar{q} \rightarrow b\bar{b}$ contribution by factor 18, but the QCD $\rightarrow b\bar{b}$ contribution by factor 12 only. Also requirements which is dedicated to suppress events with non-isolated $E_{\mathrm{T}}^{\mathrm{miss}}$ *i.e.* $\Delta\phi(E_{\mathrm{T}}^{\mathrm{miss}}, j) > 0.5$ reduces $gg, q\bar{q} \rightarrow b\bar{b}$ by factor 40 but QCD $\rightarrow b\bar{b}$ only by factor 10, see Figs. 1-4.

This rather steep behaviour with selection criteria strongly supports conclusions that the firm estimation of this background can be made only with the full detector simulation. Fast simulation, as applied here can be only used to indicate the order of the magnitude of expected background and would very likely underestimate its level.

The QCD background is overwhelming for the ZH channel. The additional selection slightly increases signal-to-background ratio (*e.g.* from 3.6% to 3.8% for $E_{\mathrm{T}}^{\mathrm{miss}} > 40$ GeV) but reduces $S/\sqrt{B}$ (res. from 1.4 to 1.3 for $E_{\mathrm{T}}^{\mathrm{miss}} > 40$ GeV).

TABLE XXXVII

The expected number of $gg, q\bar{q} \to b\bar{b}$, QCD $\to b\bar{b}$ and QCD $\to jb$ events for an integrated luminosity of 30 fb^{-1} and 2 TeV $p\bar{p}$. b-tagging efficiency and mass window acceptance is not included. In parenthesis given is fraction of events with true missing energy of $E_{\rm T}^{\nu} > 30$ GeV.

Selection	$E_{\rm T}^{\rm miss} >$			
	30 GeV	35 GeV	40 GeV	50 GeV
	$gg, q\bar{q} \to b\bar{b}$			
bb-labelled pair (10^5)	14.0 ± 0.04 (50%)	6.2 ± 0.02 (75%)	3.0 ± 0.01 (90%)	0.8 ± 0.003 (98%)
$\Delta\phi(E_{\rm T}^{\rm miss}, j) > 0.5$ (10^3)	35.0 ± 1.0 ($8.7 \pm 0.45\%$)	12.0 ± 0.5 ($16.2 \pm 1.0\%$)	3.8 ± 0.2 ($27 \pm 2\%$)	0.5 ± 0.07 ($57 \pm 8\%$)
jet-veto	26000 ± 870 ($4.8 \pm 0.4\%$)	8600 ± 490 ($9.6 \pm 1.1\%$)	2700 ± 200 ($17.3 \pm 2.4\%$)	320 ± 62 ($48 \pm 10\%$)
lepton-veto	21000 ± 750 ($4.4 \pm 0.4\%$)	6400 ± 420 ($8.3 \pm 1.1\%$)	1800 ± 170 ($15 \pm 2.7\%$)	160 ± 50 ($32 \pm 10\%$)
additional cuts	9600 ± 600 ($2.2 \pm 0.5\%$)	3400 ± 370 ($3.1 \pm 0.9\%$)	860 ± 120 ($7.8 \pm 2.8\%$)	100 ± 50 ($24 \pm 14\%$)
	QCD $\to b\bar{b}$			
bb-labelled pair (10^5)	46 ± 0.9 (50%)	22 ± 0.5 (73%)	12 ± 0.3 (87%)	4 ± 0.2 (96%)
$\Delta\phi(E_{\rm T}^{\rm miss}, j) > 0.5$ (10^3)	450 ± 34 ($22 \pm 3\%$)	190 ± 18 ($48 \pm 7\%$)	100 ± 13 ($73 \pm 11\%$)	61 ± 10 ($90 \pm 16\%$)
jet-veto (10^3)	270 ± 28 ($14.4 \pm 3.4\%$)	100 ± 15 ($38 \pm 9\%$)	49 ± 10 ($68 \pm 18\%$)	32 ± 9 ($97 \pm 30\%$)
lepton-veto (10^3)	190 ± 25 ($6.4 \pm 3\%$)	59 ± 11 ($21 \pm 9\%$)	18 ± 6 ($47 \pm 28\%$)	8 ± 5 ($97 \pm 64\%$)
additional cuts (10^3)	140 ± 18 ($3.0 \pm 0.4\%$)	44 ± 9 ($18 \pm 11\%$)	15 ± 6 ($49 \pm 33\%$)	8 ± 5 ($97 \pm 66\%$)
	QCD $\to jb$			
jb-labelled pair (10^5)	130 ± 2 (32%)	60 ± 1 (51%)	28 ± 0.7 (67%)	7.4 ± 0.3 (89%)
$\Delta\phi(E_{\rm T}^{\rm miss}, j) > 0.5$ (10^5)	43 ± 1.3 ($10 \pm 1\%$)	18 ± 0.8 ($19 \pm 2\%$)	8 ± 0.6 ($32 \pm 4\%$)	1.7 ± 0.2 ($74 \pm 12\%$)
jet-veto (10^5)	15 ± 1 ($1.3 \pm 0.2\%$)	5.4 ± 0.5 ($0.9 \pm 0.2\%$)	2.4 ± 0.4 ($0.8 \pm 0.2\%$)	0.5 ± 0.1 ($0.4 \pm 0.1\%$)
lepton-veto (10^5)	8.4 ± 0.7 ($9.6 \pm 2.5\%$)	2.7 ± 0.4 ($18 \pm 6\%$)	0.9 ± 0.2 ($44 \pm 17\%$)	0.2 ± 0.1 ($94 \pm 56\%$)
additional cuts (10^5)	7.5 ± 0.7 ($10.5 \pm 3.0\%$)	2.4 ± 0.4 ($19 \pm 6.4\%$)	0.8 ± 0.2 ($42 \pm 17\%$)	0.2 ± 0.1 ($95 \pm 57\%$)

TABLE XXXVIII

For an integrated luminosity of 30 fb^{-1}, the expected number of the ZH signal and QCD bb and jb background events in 2 TeV $p\bar{p}$ collision. The b-tagging efficiency and mass window acceptance are included. QCD background was estimated only from the sample generated with $p_{\mathrm{T}}^{\mathrm{hard}} > 30$ GeV.

Selection	$E_{\mathrm{T}}^{\mathrm{miss}} >$			
	30 GeV	35 GeV	40 GeV	50 GeV
Signal	52	50	45	40
QCD $\to b\bar{b}$	12500 $\pm$ 1600	4500 $\pm$ 800	1300 $\pm$ 400	550 $\pm$ 150
QCD $\to jb$	1000 $\pm$ 100	350 $\pm$ 50	100 $\pm$ 30	30 $\pm$ 15
S/B	0.4%	1.2%	3.6%	7.0%
$S/\sqrt{B}$	0.6	0.8	1.4	1.7

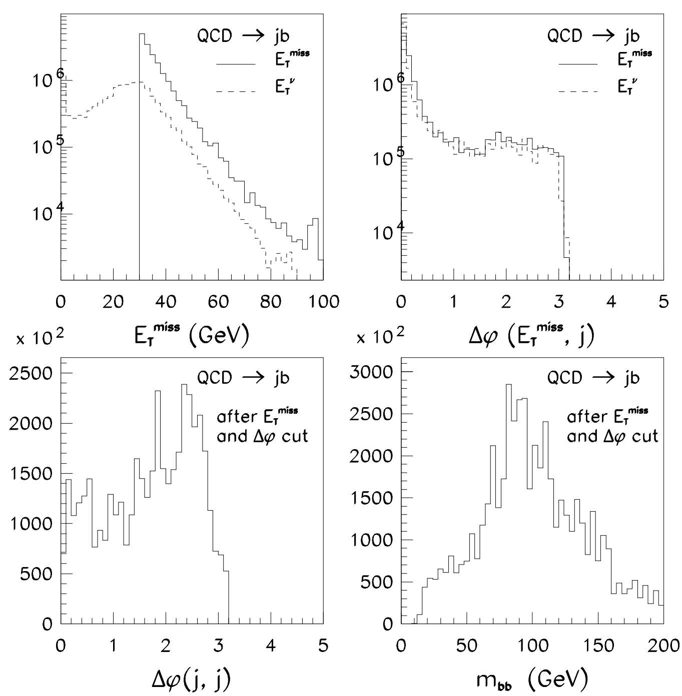

Fig. 4. The same as Fig 2 but for QCD $\to jb$ events.

5.7. Conclusions

The detailed comparison of the accessibility of the WH/ZH channels with $E_{\mathrm{T}}^{\mathrm{miss}} + b\bar{b}$ signature was presented for the 14 TeV pp and 2 TeV $p\bar{p}$ scenarios. If only background processes with W and Z in the final state were contributing, significance would be comparable in both scenarios, of 3σ for an integrated luminosity 30 fb^{-1}. For 14 TeV scenario expected signal rates are 4 times higher and expected resonant background rates 5.5 times higher, giving less favourable signal-to-resonant-background ratio. The signal-to-background ratio is higher by factor 5 for 2 TeV $p\bar{p}$ scenario.

The QCD reducible background is, with presented analysis, overwhelming for the 14 TeV scenario and a dominant one for the 2 TeV scenario. It is at least 5 times higher in 2 TeV $p\bar{p}$ and 50 times higher in 14 TeV pp collisions than the irreducible background from W and Z (for $E_{\mathrm{T}}^{\mathrm{miss}} > 35$ GeV). After this background is included, the final expected significance is reduced below 2σ for 2 TeV $p\bar{p}$ and below 1σ for 14 TeV pp.

Let us stress that the above results are optimistic as $E_{\mathrm{T}}^{\mathrm{miss}}$ reconstruction was simulated with the fast simulation only. On the other hand, further refined selection for the discrimination of the non isolated $E_{\mathrm{T}}^{\mathrm{miss}}$ would be possible with the more complete experimental analysis.

5.8. Comparison with results from [2]

Results shown in the previous section can be directly compared with these presented in the report of the Higgs Working Group of Tevatron [2]. Although [2] is not yet officially published, results from this report were publicly presented already several times [12], including recent presentation [13]. Therefore we consider them to be mature enough to justify performed below comparison. Two different analyses are reported in [2], based on the so called *QFL* and *SHW* simulations of the detector performance. The proposed selection criteria also differ in some details between both analyses, leading however to the comparable estimated signal significances in both cases. In Table XXXIX the detailed comparison between studies performed here and these reported in [2] for the SHW analysis is shown for an integrated luminosity of 30 fb^{-1}. There are obvious differences in the assumptions concerning expected detector performance. The main ingredients of the expected detector performance are $E_{\mathrm{T}}^{\mathrm{miss}}$ resolution, assumptions concerning b-tagging efficiency and non-b jets rejection and efficiencies for the jets reconstruction and jet veto. The 10% mass resolution was assumed for background estimates as used in the Tevatron report in the quoted SHW analysis.

TABLE XXXIX

Comparison between *This study* (A), *This study scaled* (A') and Tevatron report (B) (numbers are taken from Table 16 in Section C of [2]). In (B) QCD background is estimated as 100% of total $W/Z/t\bar{t}$ originated background.

Process	This study (A) 80–120 GeV	This study scaled (A') 80–120 GeV	Tevatron report (SHW study) (B) 80–125 GeV	Ratio (A')/(B)
ZH	57	142	117	1.2
WH	25	62	87	0.7
Total signal	82	204	201	1.0
ZZ	104	260	240	1.1
WZ	42	105	177	0.6
Total reson. bgd	146	365	417	0.9
tt	48	120	216	0.5
single t	26	65	240	0.3
Wbb	150	375	234	1.6
Wjj (other)	50	50	none	—
Zbb	395	990	309	3.2
Zjj (other)	36	36	none	—
Total cont. bgd (W, Z, t, $t\bar{t}$)	705	1600	1000	1.6
Total bgd (W, Z, t, $t\bar{t}$)	850	2000	1400	1.4
$S/\sqrt{B}$	2.8	4.6	5.3	0.9
S/B	9.6%	10%	14%	0.7
		not scaled		
QCD ($b\bar{b}$)	4500 ± 800	4500 ± 800	1400(?)	3.0
QCD (other)	350 ± 50	350 ± 50	none	—
Total bgd	5700 ± 850	6850 ± 850	2800 (?)	2.4
$S/\sqrt{B}$	1.1	2.5	3.8 (?)	0.6
S/B	1.4%	3%	7% (?)	0.4

- For *This study* performance as expected for the ATLAS detector at LHC is assumed[6] following however the selection criteria as proposed in the Tevatron report. This includes reduced pseudorapidity coverage and softer jet veto, as already used in Section 3. In addition to the selection criteria specified so far, the requirement $\Delta\phi(E_{\rm T}^{\rm miss}, {\rm jet}) > 0.5$ is used as in the analysis presented in [2].
- For *This study scaled* the efficiency for double b-tag was rescaled[7] for signal and physics backgrounds to reproduce that efficiency reported for the signal events in [2]. The necessary scaling factor was 2.5. In the similar case of the $\ell b\bar{b}$ analysis, respective needed scaling factor was 1.7 only [3]. The QCD background was not rescaled.

There are several inconsistencies in the background estimates from different channels between study performed here and this reported in [2].

- The total signal and resonant background rates are predicted in [2] to be consequently higher by factor 2, which comes mostly from the higher assumed acceptance for double b-tag.
- Predicted rates for the continuum background from W, Z, t, $t\bar{t}$ are in agreement, which is rather accidental, as it comes from compensation of the effect of neglecting Wjj and Zjj reducible backgrounds and predicting much higher t and $t\bar{t}$ background in [2]. This accidental agreement is also misleading as the assumed performance on the double b-tag is higher by factor 2 in [2] (compare respective entries in *This study* and *This study scaled*) so the similar ratio of 2 should holds also for the total irreducible background.
- The QCD background, from estimates presented in this paper, is at least 5 times higher than the total W, Z, t, $t\bar{t}$ background. It was considered negligible for the long time in the studies of Tevatron [2, 12]. Only recently, it was included in the final estimates [2, 13] as being on the level of the total W, Z, t, $t\bar{t}$ background.

Estimates for the QCD background in [2] were obtained extrapolating results from the CDF Run I Higgs search. It is argued further there, that with the tighter selection criteria it will be possibly to suppress this background even more efficiently. A point is also made that this background is very unreliable for simulation with presently available Monte Carlo generators.

Let us stress that more substantial than assumed in [2] contribution from this background, which is indicated by results from the Monte Carlo simulation presented here, would drastically change prospects for the observability of the $E_{\rm T}^{\rm miss} + b\bar{b}$ signature in 2 TeV $p\bar{p}$ collision.

[6] *Eg.* the $E_{\rm T}^{\rm miss}$ was reconstructed for assumed ATLAS coverage of the detector *i.e.* calorimetric coverage up to $|\eta| < 5.0$ and muon reconstruction up to $|\eta| < 2.5$.

[7] We could not use directly parametrisation for the b-tagging efficiency given in [2], as the information on the reconstruction efficiency for b-labelled pair was not available there.

TABLE XL

Break-down of partial acceptances for estimates given in Table XXXIX. For *Tevatron report* column they are extracted from the Table 15 and 16 in Section C of [2].

Process	This study (A)	Tevatron report (SHW study) (B)	Comments
	ZH $(Z \to \nu\nu)$ signal		
$\sigma \times BR$ (pb)	0.023	0.027	factor 1.2 higher σ in (B)
Double b-tag	17.2%	43%	includes also jets reconstruction
$E_{\rm T}^{\rm miss}$>35 GeV	72.1%	72%	
$\Delta\phi(E_{\rm T}^{\rm miss}, {\rm jet})$	90.0%	91%	
Jet veto	86.1%	77%	scalar hadronic energy sum used instead in (B)
Lepton veto	100%	90%	why so low in (B)?
Mass window	85.0%	73.6%	$\pm$ 10 GeV window used in (B) ?? 80–120 GeV in (A)
Total accept	8.1%	14.4%	
Expected events	57	117	2.1 times higher rates in (B)
	ZH $(Z \to \tau\tau)$ signal		
$\sigma \times BR$ (pb)	0.0039		
Expected events	1		
	WH $(W \to \ell\nu(e, \mu, \tau))$ signal		
$\sigma \times BR$ (pb)	0.064	0.071	
Double b-tag	16.7%	39.9%	includes also jets reconstruction
$E_{\rm T}^{\rm miss}$>35 GeV	57.0%	62.3%	
$\Delta\phi(E_{\rm T}^{\rm miss}, {\rm jet})$	82.5%	88.2%	
Jet veto	82.2%	54.0%	scalar hadronic energy sum used instead in (B)
Lepton veto	27.0%	43.8%	only $W \to \ell\nu$ included in (B)
Mass window	85%	74.4%	$\pm$ 10 GeV window used in (B) ?? 80–120 GeV in (A)
Total accept	1.3%	3.9%	
Expected events	25	87	2.5 times higher rates in (B)

TABLE XLI

Continuation of Table XL.

Process	This study (A)	Tevatron report (SHW study) (B)	Comments
	ZZ ($Z \to \nu\nu$) background		
$\sigma \times BR$ (pb)	0.068	0.137	missprint in (B) ??
Double b-tag	14.4%	34.8%	includes also jets reconstruction
$E_{\rm T}^{\rm miss} > 35$ GeV	58.9%	38.6%	
$\Delta\phi(E_{\rm T}^{\rm miss}, {\rm jet})$	90.7%	89.3%	
Jet veto	87.0%	79.5%	scalar hadronic energy sum used instead in (B)
Lepton veto	99.9%	91.2%	why so low in (B)?
Mass window	75.0%	67.6%	$\pm$ 10 GeV window used in (B) ?? 80–120 GeV in (A)
Total accept	5.0%	5.9%	
Expected events	102	240	2.3 times higher rates in (B)
	ZZ ($Z \to \tau\tau$) background		
$\sigma \times BR$ (pb)	0.0114		
Expected events	2		
	ZZ ($Z \to \ell\ell$) background		
$\sigma \times BR$ (pb)	0.0228		
Expected events	<0.05		
	WZ ($W \to \ell\nu(e,\mu,\tau)$) background		
$\sigma \times BR$ (pb)	0.123	0.135	missprint in (B) ??
Double b-tag	13.0%	32.2%	includes also jets reconstruction
$E_{\rm T}^{\rm miss} > 35$ GeV	55.5%	57.5%	
$\Delta\phi(E_{\rm T}^{\rm miss}, {\rm jet})$	82.7%	90.3%	
Jet veto	70.7%	68.5%	scalar hadronic energy sum used instead in (B)
Lepton veto	36.0%	50.0%	why so low in (B)?
Mass window	75.0%	66.8%	$\pm$ 10 GeV window used in (B) ?? 80–120 GeV in (A)
Total accept	1.1%	4.4%	
Expected events	42	180	4.3 times higher rates in (B)

TABLE LXII

Continuation of Table XL.

Process	This study (A)	Tevatron report (SHW study) (B)	Comments
	$Zbb(Z \to \nu\nu)$ background		
$\sigma \times BR$ (pb) filtered to	360 32.3	0.668 (ME)	
Double b-tag + mass window in (A) $E_{\mathrm{T}}^{\mathrm{miss}} > 35$ GeV $\Delta\phi(E_{\mathrm{T}}^{\mathrm{miss}}, \mathrm{jet})$ Jet veto Lepton veto Mass window Total accept	0.15% 40% 85% 80% 100% already incl. 0.04%	18.5% 69.6% 90.5% 68.3% 91.6% 21.5% 1.55%	includes also jets reconstruction scalar hadronic energy sum used instead in (B) why so low in (B)? ±10 GeV window used in (B)?? 80–120 GeV window used in (A)
Expected events	395	309	not all graphs in (A)
	Wbb background with $W \to \ell\nu(e, \mu, \tau)$		
$\sigma \times BR$ (pb)	(PYTHIA) only $W \to \ell\nu$ after filter	2530 (ME)	
Double b-tag + mass window in (A) $E_{\mathrm{T}}^{\mathrm{miss}} > 35$ GeV $\Delta\phi(E_{\mathrm{T}}^{\mathrm{miss}}, \mathrm{jet})$ Jet veto Lepton veto Mass window Total accept	0.07% 50.7% 76.7% 84.6% 8.7% already incl. 0.002%	11.9% 50.3% 91.3% 88.7% 41.5% 15.4% 0.31%	includes also jets reconstruction scalar hadronic energy sum used instead in (B) only $W \to \ell\nu$ in (A) ±10 GeV window used in (B)?? 80–120 GeV window used in (A)
Expected events	$50 \times 3 =$ 150	 234	only $W \to \ell\nu$ in (A) $W \to \ell\nu$ gives 31% of total

TABLE XLIII

Continuation of Table XL.

Process	This study (A)	Tevatron report (SHW study) (B)	Comments
	$t\bar{t}$ background; $W \to \ell\nu(e,\mu,\tau)$		
$\sigma \times BR$ (pb)	3.93	6.8	
Double b-tag	22.1%	44.3%	includes also jets reconstr.
$E_{\rm T}^{\rm miss} > 35$ GeV	25.9%	46.4%	
$\Delta\phi(E_{\rm T}^{\rm miss},{\rm jet})$	69.5%	87.6%	
Jet veto	66.3%	4.1%	scalar hadronic energy sum used instead in (B)
Lepton veto	16.9%	38.2%	
Mass window	39.0%	37.3%	$\pm$ 10 GeV window used in (B)?? 80–120 GeV window used in (A)
Total accept	0.044%	0.1%	
Expected events	48	216	why so high in (B)
	tq background; $W \to \ell\nu(e,\mu,\tau)$		
$\sigma \times BR$ (pb)	0.85	0.81	
Double b-tag	4.8%	9.1%	includes also jets reconstr.
$E_{\rm T}^{\rm miss} > 35$ GeV	64.3%	73.2%	
$\Delta\phi(E_{\rm T}^{\rm miss},{\rm jet})$	76.2%	90.2%	
Jet veto	23.6%	49.9%	scalar hadronic energy sum used instead in (B)
Lepton veto	32.3%	54.3%	
Mass window	30.4%	21.5%	$\pm$ 10 GeV window used in (B)?? 80–120 GeV window used in (A)
Total accept	0.11%	0.35%	
Expected events	14	85	

TABLE XLIV

Continuation of Table XL.

Process	This study (A)	Tevatron report (SHW study) (B)	Comments
	$W^* \to tb$ background		
$\sigma \times BR$ (pb)	0.11 $W \to \ell\nu(e,\mu)$	1.0 $W \to \ell\nu(e,\mu,\tau)$	
Double b-tag	27.5%	32.3%	includes also jets reconstr.
$E_{\mathrm{T}}^{\mathrm{miss}} > 35$ GeV	68.4%	27.6%	
$\Delta\phi(E_{\mathrm{T}}^{\mathrm{miss}}, \mathrm{jet})$	85.0%	88.5%	
Jet veto	82.5%	40.7%	scalar hadronic energy sum used instead in (B)
Lepton veto	6.3%	49.5%	
Mass window	28.7%	32.3%	$\pm$ 10 GeV window used in (B)?? 80–120 GeV window used in (A)
Total accept	0.24%	0.51%	
Expected events	$8 \times 1.5 =$ 12	155	only $W \to \ell\nu$ in (A) 3 time higher accept. for $W \to \tau\nu$

6. Conclusions

The primary aim of this paper was to discuss the origin of the differences in the expected potential for the Higgs boson discovery in the WH/ZH production, with $H \to b\bar{b}$ and $E_{\mathrm{T}}^{\mathrm{miss}} + b\bar{b}$ signature, in 2 TeV $p\bar{p}$ and 14 TeV pp collisions.

This signature is considered as not accessible at LHC [1], but a more quantitative evaluation of the expected rates is presented for the first time in this paper. The sensitivity was confirmed to be hopeless because of the overwhelming background from the QCD di-jet production. Even if only background from W, Z, $t\bar{t}$ were present, the expected sensitivity would be on the same level as for the WH channel with the $\ell b\bar{b}$ signature [3], namely around 3σ for an integrated luminosity of 30 fb^{-1}.

A detailed comparison of the expected signal and background at 14 TeV pp and 2 TeV $p\bar{p}$ was carried out assuming the same performance of the detector and ATLAS or Tevatron like selection criteria (geometrical acceptances, jet-veto requirements). The results obtained here for 2 TeV $p\bar{p}$ are much less optimistic than those presented in the Tevatron report [2].

- In the studies presented here the signal rates are estimated to be 2.4 times lower. The background rates from W or Z in the final state are simulated to be comparable to those estimated in [2].
- The QCD background, estimated here from the Monte Carlo simulation, was found to be almost 5 times higher than the total background from the W and Z. In the recent version of [2] it is included at the level of 100% of the total background from the W and Z, based on the extrapolation from the CDF Run I Higgs searches. In [2] it is pointed out that this background is considered to be very unreliable to be estimated from the Monte Carlo simulation.

The fact that WH/ZH channel with $E_{\rm T}^{\rm miss} + b\bar{b}$ signature might be overwhelmed by QCD background would substantially reduce not only the prospects for the observability of this channel alone but also the overall potential for the Higgs searches at the Tevatron as presented in [2].

This work has been done in the framework of the ATLAS Collaboration, to which I am grateful for very valuable inputs and discussions.

In particular, it presents an extension and continuation of the previous study done with Daniel Froidevaux and documented in [6]. I would like to thank him very warmly for valuable suggestions and inspiring discussions which guided the present study. I am also grateful to Fabiola Gianotti and Karl Jakobs for several very constructive critical comments.

REFERENCES

[1] ATLAS Collaboration, ATLAS Detector and Physics Performance Technical Design Report, CERN/LHCC/99-14, ATLAS TDR 14, 25 May 1999.

[2] Report of the Physics at RUN II Supersymmetry/Higgs Workshop, Fermilab, 1999, eds. M. Carena and J. Lykken, in preparation, draft version from http://fnth37.fnal.gov/higgs/draft.html, 30 November 1999; J. Conway, 'Higgs Discovery Potential in Run II at Tevatron', conference talks, La Thuile, 3 March 1999; Sitges, 30 April 1999; M. Carena, 'Beyond the Standard Model', conference talk at IEC HEP, Tampere'99, 20 July, 1999.

[3] E. Richter-Wąs, *Acta Phys. Pol.* **B31**, 1931 (2000).

[4] ATLAS Collaboration, ATLAS Technical Proposal, CERN/LHCC/94-43, 15 December 1994.

[5] E. Richter-Wąs, M. Sapinski, ATLAS Note ATL-PHYS-98-132 (1998).

[6] D. Froidevaux, E. Richter-Wąs, ATLAS Note ATL-PHYS-94-043 (1994), *Z. Phys.* **C67**, 213 (1995).

[7] E. Richter-Wąs, D. Froidevaux, L. Poggioli, ATLAS Note ATL-PHYS-98-131 (1998).

[8] ATLAS Collaboration, ATLAS Inner Detector Technical Design Report, CERN/LHCC/98-13.

[9] B. van Eijk, R. Kleiss, in Proceedings of the Large Hadron Collider Workshop, Aachen, 1990, edited by G. Jarlskog and D. Rein, CERN 90-10/ECFA 90-133, p. 183.

[10] ATLAS Collaboration, ATLAS Trigger Performance Status Report, LHCC 98-15, June 1998.

[11] ATLAS Collaboration, ATLAS Calorimeter Performance Technical Design Report, CERN/LHCC/96-40, December 1996 .

[12] *e.g.* J. Conway, Searching for the Higgs in Run 2 at the Tevatron, presentation on SUSY-99 Conference, Fermilab, June 14, 1999; M. Carena, Higgs Physics at Tevatron Collider, XXXIVnd Rencontres de Moriond, Les Arcs, France, on March 17, 1999; M.P.T. Roco, Prospects for the Higgs Discovery at the Tevatron, presented on EPS-HEP99, Tampere, Finland, 15 July 1999.

[13] J. Conway, Prospects for Higgs Searches at the Tevatron, talk given on the LHCC open session, CERN, 5 July 2000.